National Library of Canada
Bibliothèque nationale du Canada

Canadian Theses Service
Services des thèses canadiennes

Ottawa, Canada
K1A 0N4

CANADIAN THESES
THÈSES CANADIENNES

NOTICE

The quality of this microfiche is heavily dependent upon the quality of the original thesis submitted for microfilming. Every effort has been made to ensure the highest quality of reproduction possible.

If pages are missing, contact the university which granted the degree.

Some pages may have indistinct print especially if the original pages were typed with a poor typewriter ribbon or if the university sent us an inferior photocopy.

Previously copyrighted materials (journal articles, published tests, etc.) are not filmed.

Reproduction in full or in part of this film is governed by the Canadian Copyright Act, R.S.C. 1970, c. C-30. Please read the authorization forms which accompany this thesis.

AVIS

La qualité de cette microfiche dépend grandement de la qualité de la thèse soumise au microfilmage. Nous avons tout fait pour assurer une qualité supérieure de reproduction.

S'il manque des pages, veuillez communiquer avec l'université qui a conféré le grade.

La qualité d'impression de certaines pages peut laisser à désirer, surtout si les pages originales ont été dactylographiées à l'aide d'un ruban usé ou si l'université nous a fait parvenir une photocopie de qualité inférieure.

Les documents qui font déjà l'objet d'un droit d'auteur (articles de revue, examens publiés, etc.) ne sont pas microfilmés.

La reproduction, même partielle, de ce microfilm est soumise à la Loi canadienne sur le droit d'auteur, SRC 1970, c. C-30. Veuillez prendre connaissance des formules d'autorisation qui accompagnent cette thèse.

THIS DISSERTATION
HAS BEEN MICROFILMED
EXACTLY AS RECEIVED

LA THÈSE A ÉTÉ
MICROFILMÉE TELLE QUE
NOUS L'AVONS REÇUE

Canada

NL 339 (r. 86/01)

108

0-315-26841-7

National Library of Canada | Bibliothèque nationale du Canada

Canadian Theses Division | Division des thèses canadiennes

Ottawa, Canada
K1A 0N4

PERMISSION TO MICROFILM — AUTORISATION DE MICROFILMER

• Please print or type — Écrire en lettres moulées ou dactylographier

Full Name of Author — Nom complet de l'auteur

DAVID ALLEN SCHWAB

Date of Birth — Date de naissance

June 29, 1958

Country of Birth — Lieu de naissance

USA

Permanent Address — Résidence fixe

1450 DREON DRIVE
CLAWSON, MI
USA 48017

Title of Thesis — Titre de la thèse

Design of a CCD Spectrophotometer for Spectroelectrochemical Studies

University — Université

UNIV. OF ALBERTA

Degree for which thesis was presented — Grade pour lequel cette thèse fut présentée

MASTER'S

Year this degree conferred — Année d'obtention de ce grade

1983

Name of Supervisor — Nom du directeur de thèse

Dr. B. STAN PONS

Permission is hereby granted to the NATIONAL LIBRARY OF CANADA to microfilm this thesis and to lend or sell copies of the film.

The author reserves other publication rights, and neither the thesis nor extensive extracts from it may be printed or otherwise reproduced without the author's written permission.

L'autorisation est, par la présente, accordée à la BIBLIOTHÈQUE NATIONALE DU CANADA de microfilmer cette thèse et de prêter ou de vendre des exemplaires du film.

L'auteur se réserve les autres droits de publication; ni la thèse ni de longs extraits de celle-ci ne doivent être imprimés ou autrement reproduits sans l'autorisation écrite de l'auteur.

Date

June 27, 1983

Signature

David A. Schwab

NL-91 (4/77)

THE UNIVERSITY OF ALBERTA

DESIGN OF A CCD SPECTROPHOTOMETER FOR SPECTROELECTROCHEMICAL STUDIES

by

(C) DAVID ALLEN SCHWAB

A THESIS

SUBMITTED TO THE FACULTY OF GRADUATE STUDIES AND RESEARCH

IN PARTIAL FULFILMENT OF THE REQUIREMENTS FOR THE DEGREE

MASTER OF SCIENCE

DEPARTMENT OF CHEMISTRY

EDMONTON, ALBERTA

FALL 1983

THE UNIVERSITY OF ALBERTA

RELEASE FORM

NAME OF AUTHOR David Allen Schwab

TITLE OF THESIS Design of a CCD Spectrophotometer for Spectroelectrochemical Studies

DEGREE FOR WHICH THESIS WAS PRESENTED M.Sc.

YEAR THIS DEGREE GRANTED 1983

Permission is hereby granted to THE UNIVERSITY OF ALBERTA LIBRARY to reproduce single copies of this thesis and to lend or sell such copies for private, scholarly or scientific research purposes only.

The author reserves other publication rights, and neither the thesis nor extensive extracts from it may be printed or otherwise reproduced without the author's written permission.

(Signed) David A. Schwab

PERMANENT ADDRESS:

1450 Dreon Drive
Clawson, MI
48017

DATED June 27 19 83

THE UNIVERSITY OF ALBERTA

FACULTY OF GRADUATE STUDIES AND RESEARCH

The undersigned certify that they have read, and recommend to the Faculty of Graduate Studies and Research, for acceptance, a thesis entitled DESIGN OF A CCD SPECTRO-PHOTOMETER FOR SPECTROELECTROCHEMICAL STUDIES.....

.....

submitted by DAVID ALLEN SCHWAB.....

in partial fulfilment of the requirements for the degree of

Master of Science.....

.....

R. A. Locock

James A. Plambeck

DATE June 23, 1983

TO MY MOM AND DAD

ABSTRACT

In this study, specular reflectance spectroscopy was carried out in the u.v.-visible region using a new detector, a charge-coupled device. This new detector enabled the reflectance experiment to be performed while monitoring an electrogenerated species simultaneously over a relatively large wavelength range. The charge-coupled device also allowed for a substantial simplification in the electronic circuitry required to perform reflectance experiments as opposed to the commonly used photomultiplier tube.

The interfacing of the new detector to an AIM 65/6502 microprocessor is detailed along with the operation of such a system and its accompanying electronic circuitry during a reflectance experiment. A qualitative description of the charge-coupled device is also given after which its superiority over the more common photodiode array is inferred.

This work demonstrates the ease with which the usual two dimensional reflectance information could be expanded to contain wavelength as the third dimension.

ACKNOWLEDGEMENTS

I would like to thank Dr. B. Stanley Pons for the opportunity to carry out this research and for his invaluable guidance throughout this project.

I wish to thank Debbie for all her patience and the never ending T.L.C. she provided throughout my studies.

I wish also to thank Martin Dubetz for his helpful ideas dealing with the electronic system.

Finally, I would like to thank the Electronics Shop for their prompt and courteous services.

TABLE OF CONTENTS

Dedication..... iv

Abstract..... v

Acknowledgements..... vi

List of Tables..... ix

List of Figures..... x

CHAPTER PAGE

1. INTRODUCTION..... 1

2. THEORY..... 9

3. EXPERIMENTAL..... 24

3.1 Preparations and Purifications..... 24

3.1.1 Purification of Acetonitrile..... 24

3.2 Supporting Electrolytes..... 26

3.2.1 Preparation of Tetra-n-butylammonium Tetrafluoroborate..... 26

3.2.2 Purification of Lithium Perchlorate.. 27

3.3 Commercial Chemicals..... 28

3.4 Optical Reflectance Cell and Electrodes..... 28

3.5 Experimental Apparatus..... 34

3.6 Array Detectors..... 55

CHAPTER PAGE

4. RESULTS AND DISCUSSION..... 66

4.1 Conclusion..... 90

***

BIBLIOGRAPHY..... 92

APPENDIX A..... 100

LIST OF TABLES

TABLE	PAGE
1. MSRS data obtained with a PMT vs. a CCD.....	81

LIST OF FIGURES

FIGURE		PAGE
1.	a) Internal reflection. b) Transmission. c) Specular reflectance.....	2
2.	Light path geometry of reflectance cell.....	22
3.	Optical working electrode.....	29
4.	Polishing mandril for the optical working electrode.....	31
5.	Optical reflectance cell.....	33
6.	Experimental apparatus used to perform reflectance experiments.....	35
7.	Block diagram of electronic system.....	37
8.	Synchronized clock signals.....	38
9.	CCD and on-board circuitry.....	41
10.	Counter circuitry.....	43
11.	Signal processing circuitry.....	44
12.	Timing diagram for loading of decade counters...	48
13.	Timing diagram for electronic system operation..	49
14.	Decade counters.....	50
15.	a) MOS Capacitor. b) Potential well with signal.....	56

FIGURE PAGE

16. a) 3-phase n-channel CCD.
b,c,d) Potential wells depicting the transfer of charge.
e) Associated timing diagram..... 58
17. Buried channel CCD..... 60
18. Bilinear arranged BCCD..... 62
19. PDA schematic..... 63
20. Experimental apparatus used to perform reflectance experiments with a PMT..... 67
21. PMT feedback circuit..... 69
22. Cyclic voltammogram of 2,6-di-tert-butyl-4-(4-methoxyphenyl)-aniline..... 74
23. Spectrum of the 2,6-di-tert-butyl-4-(4-methoxyphenyl)-aniline cation radical obtained with a CCD..... 75
24. Spectrum of the 2,6-di-tert-butyl-4-(4-methoxyphenyl)-aniline cation radical obtained with a PMT..... 76
25. Concentration profile of an electrogenerated species vs. time..... 79
26. Cyclic voltammogram of 1,4-dimethoxy-9,10-diphenylanthracene..... 83
27. Spectrum of the 1,4-dimethoxy-9,10-diphenylanthracene cation radical (60-65 ms).... 84

FIGURE PAGE

28. Spectrum of the 1,4-dimethoxy-9,10-diphenylanthracene cation radical (45-50 ms).... 85

29. Spectrum of the 1,4-dimethoxy-9,10-diphenylanthracene cation radical (30-35 ms).... 86

30. Spectrum of the 1,4-dimethoxy-9,10-diphenylanthracene cation radical (15-20 ms).... 87

31 Spectrum of the 1,4-dimethoxy-9,10-diphenylanthracene cation radical (0-5 ms)..... 88

32. Plot of ΔR/R vs. the duration of the integration period..... 89

CHAPTER 1

INTRODUCTION

In recent years, spectroscopy has been utilized to augment many of the electrochemical techniques [1,2]. The basic spectroscopic methods used include internal reflection (Figure 1a), transmission (Figure 1b), and specular reflectance (Figure 1c). The coupling of any one of these spectroscopic methods to an electrochemical technique can be accomplished by spectroscopically monitoring the region close to the electrode/solution interface as the potential of the electrode is changed from a reference region of electrochemical activity to one where a different electrochemical activity is apparent. Through such a combination the resulting electrochemical information is enhanced due to the molecular specificity imparted by the spectroscopic observation of the species of interest. The basic premise underlying this spectroelectrochemical combination is, of course, that the species of interest has a net absorbance difference at two potentials with this net difference being distinguishable from any background present at the wavelength of monitoring. The successful coupling of these techniques

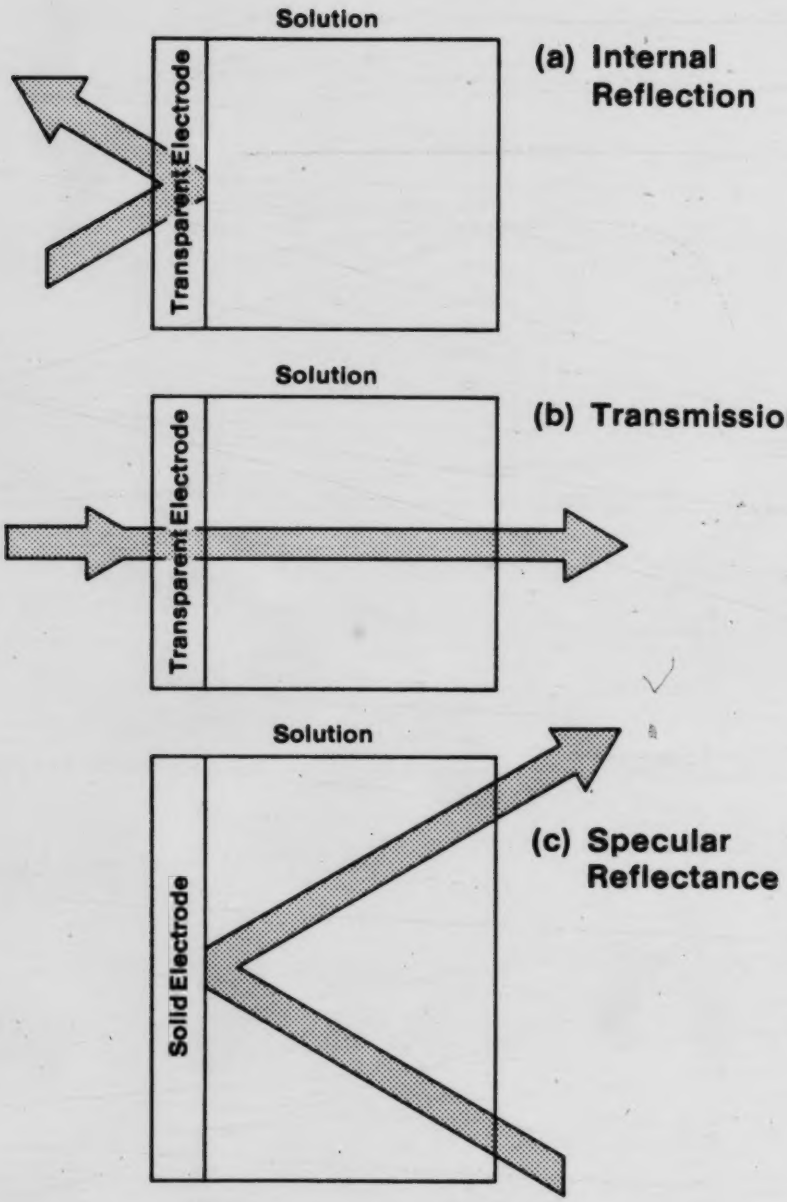
Solution
Transparent Electrode
(a) Internal Reflection
Solution
Transparent Electrode
(b) Transmission
Solution
Solid Electrode
(c) Specular Reflectance

Figure 1.

alone has resulted in the acquisition of some heretofore unattainable electrochemical information. The acquisition of such data gives justification for at least a qualitative discussion on the implementation of these three basic techniques.

In internal reflection spectroscopy [3-15], which was initially applied to spectroelectrochemistry in 1966 [3], the beam of light is incident on the back side of an optically transparent electrode (OTE) at an angle greater than the critical angle resulting in the total reflection of the light beam. The electric field associated with the totally reflected light beam forms a standing wave perpendicular to the surface. This wave extends slightly past the electrode's inner surface and into the solution where its electric field decays exponentially. Due to this evanescent wave, any electrogenerated species which is able to interact with the electric field is amenable to spectral monitoring via this technique. The penetration depth of the electric field, which is dependent both on the optical constants of the solution and the wavelength of the incident light, is usually about one-tenth this wavelength. Due to this small penetration depth, this technique is limited to investigations dealing with species essentially residing at the electrode/solution interface. The limited penetration depth can also impose

severe restrictions on the maximum duration of such an experiment due to the fast acquisition of a steady state caused by a decrease in the rate of change of the diffusional processes occurring at the electrode's surface. The sensitivity of this technique can be increased through the use of multiple reflections.

In transmission spectroscopy [16-24], the beam of light is passed directly through an OTE and the accompanying solution. By monitoring the change in transmittance of the light beam as the potential of the OTE is stepped into the electroactive region, the properties of the electrogenerated species can be evaluated. These properties include the molar absorptivity (ε), the diffusion coefficient (D_0), and more importantly, in terms of mechanistic studies, the rate of formation or decay of the absorbing electrogenerated species. If the wavelength is scanned as the potential is stepped, the spectrum of an electrogenerated species can also be acquired. Many of the OTE's (25) used in transmission spectroscopy are made by chemical vapor deposition of a very thin layer of platinum, silver, gold, tin oxide, or indium oxide on a substrate whose composition is determined by its optical transparency over the wavelength range of interest. Since the initial introduction of the electrochemical technique utilizing

transmission spectroscopy in 1964 by Kuwana et al. [16], this technique has become well characterized and quite diverse in its applications.

In specular reflectance spectroscopy [26-35], the incident light is first passed through the solution and then totally reflected from the surface of a solid electrode. In this increasingly popular technique, the electroactive species generated at the electrode surface is also monitored as it diffuses out into the bulk solution. This technique not only provides access to the data obtainable by transmission techniques, but by using phase sensitive detection can become very sensitive; in some cases even able to detect 10^{-17} moles/cm^2 of a substance. In another application utilizing signal averaging, kinetic information on the microsecond time scale can be acquired.

In a more recent and very specific application of specular reflectance referred to as "sinusoidally modulated alternating current reflectance spectroscopy" [36], an increase in sensitivity over electrochemical methods can be realized due to the absence of charging currents which can give quite large electrochemical backgrounds. In this technique a slowly varying cyclic potential ramp is applied to an electrode. Superimposed on the cyclic potential ramp is a small amplitude

sinusoidal perturbation which results in the production of an alternating current in the electroactive region of the species under investigation. This electroactive species is monitored spectroscopically giving the fundamental harmonic alternating components of the concurrent specular reflection response which is recorded through the use of phase sensitive detection instrumentation. Since the species is monitored spectroscopically, the charging current is not detected. Through new applications of specular reflectance along with the increase in sensitivity realized, the future acceptance and widespread use of this technique as an important analytical tool seems to be assured.

The aforementioned techniques have all proven to be valuable tools in electrochemical investigations. Valuable information has been gained in studies dealing with the structure of the electrical double layer [46-50] and evaluations of the kinetic parameters associated with faradaic processes or post-faradaic homogeneous processes in the diffusion layer [1,2,12,17,21,23,31,44,51,52], adsorption [10,11,26,37,38,39,42,43,45], metal deposition [23,24,45,53], and the identification and characterization of short lived reaction intermediates [17,19,27,28,44]. More recently, these techniques have been implemented for determinations of the stoichiometry and energetics of

biological components dealing with electron transport mechanisms [35,40,41]. Although the inclusion of any one of these techniques in an electrochemical investigation would prove to be quite valuable, it should be noted that reflectance techniques have several inherent advantages over transmission techniques using OTE's. First, the measured light intensity after transmission through an OTE can be greatly attenuated compared to that reflected from a solid electrode. This is due to the ineluctable absorbance of the thin layer conductor. Second, the path taken by the light beam in a reflection experiment traverses the double layer twice at an angle differing from that normal to the electrode surface allowing a greater number of the species of interest to be encountered which results in increased sensitivity. Third, to prevent the light path from being obstructed by the counter electrode in OTE's, it is necessary to sacrifice any arrangement that would place all points on the working electrode surface equidistant from the counter electrode. This is not a problem in reflection techniques. Fourth, the often encountered high resistivities of OTE's manufactured by metal vapor deposition or other techniques can result in uneven current distributions which are not present in reflectance techniques using pure bulk metal electrodes. Due to the

aforementioned advantages of reflectance over transmission techniques, spectroelectrochemical reflectance techniques were used exclusively in this research for the *in situ* monitoring of solution free electrogenerated intermediates. In typical reflectance techniques, the experiment is carried out and monitored at one wavelength at a time using the ubiquitous photomultiplier tube. The approach taken here is to perform these experiments, but to use a new detector that allows the simultaneous recording of an entire spectrum of dispersed light. Thus, not only does an experiment give the usual two dimensional results of potential (or time) vs. absorbance (or current) at a specific wavelength, but now we can conveniently include the third dimension of wavelength. To this end, an entirely new spectrometer system was designed and tested in this work. The device used to simultaneously record the dispersed spectrum was a charge coupled device (CCD), similar in package to the more familiar photodiode array (PDA), but inherently different in operation and characteristics. The operation of a CCD will be qualitatively described along with the interfacing of this device to an AIM 65/6502 microprocessor and external control circuitry. Applications of this new rapid spectrometer will be presented.

CHAPTER 2

THEORY

In this research, the spectroscopic equivalent of chronoamperometry was carried out using a CCD as a detector. The experimentally observable variable is $\Delta R/R$ which is the difference in the intensity of the reflected beam of light during the potential step and before the potential step, divided by the intensity before the potential step. In order to relate $\Delta R/R$ to the electrochemical variables, it is necessary to solve Fick's second law which describes the diffusion of species R during an electrochemical experiment [54]. For a simple reversible electrode process

$$O_X \underset{-ne^-}{\overset{+ne^-}{\rightleftharpoons}} Red \qquad (1)$$

Fick's second law is

$$\frac{\partial C_{Red}(x,t)}{\partial t} = D_{Red}\left\{\frac{\partial^2 C_{Red}(x,t)}{\partial x^2}\right\} \qquad (2)$$

where D_{Red} is the diffusion coefficient of species C_{Red}. The solution, $C_{Red}(x,t)$, will give the concentration profile of species C_{Red} as a function of distance, x, from the electrode surface and as a function of time, t. In this experiment we assume semi-infinite linear diffusion.

Initially the applied potential is in a region of no electrochemical activity. This potential is then stepped into a region such that the ensuing electron transfer is solely governed by the rate at which species C_{Red} diffuses to the electrode surface. The boundary conditions for such an experiment are:

1. Initial boundary condition:

$$C_{Red}(x,0) = C^*_{Red} \tag{3}$$

which states that at t = 0 the solution contains, everywhere, the bulk concentration C^*_{Red} (i.e. the concentration of C_{Red} at the electrode surface is equivalent to the bulk concentration, C^*_{Red}).

2. Semi-infinite boundary condition:

$$\lim_{x \to \infty} C_{Red}(x,t) = C^*_{Red} \tag{4}$$

which states that at any time, $t > 0$, at some distance from the electrode surface the concentration of the electroactive species will remain undisturbed and equivalent to the bulk concentration, C^{*}_{Red} (i.e., the cell is large enough to be approximated by semi-infinite linear diffusion to a planar electrode).

3. Surface boundary condition:

$$C_{Red}(0,t) = 0 \text{ for } t > 0 \qquad (5)$$

which states that upon application of the potential step, the rate of the electron transfer is governed by the rate at which the species can diffuse to the electrode surface. Therefore, the concentration of the electroactive species C_{Red} at the electrode surface is effectively zero (i.e., the electroactive species C_{Red} is being consumed as fast as it can diffuse to the electrode surface).

A solution to equation (2) can be arrived at through a straightforward application of the Laplace transform (L) [55] and the above boundary conditions. Using the differentiation theorem for the original function:

$$L\left\{\frac{\partial C_{Red}(x,t)}{\partial t}\right\} = s\left\{\bar{C}_{Red}(x,s)\right\} - C_{Red}(x,0) \qquad (6)$$

and

$$L\left\{D_{Red}\frac{\partial^2 C_{Red}(x,t)}{\partial x^2}\right\} = D_{Red}\left\{\frac{\partial^2 [LC_{Red}(x,t)]}{\partial x^2}\right\}$$

$$= D_{Red}\left\{\frac{\partial^2 \bar{C}_{Red}(x,s)}{\partial x^2}\right\} \qquad (7)$$

where $\bar{C}_{Red}(x,s)$ denotes the transformed function. The resulting image equation is

$$s\left\{\bar{C}_{Red}(x,s)\right\} - C_{Red}(x,0) = D_{Red}\left\{\frac{\partial^2 \bar{C}_{Red}(x,s)}{\partial x^2}\right\} \qquad (8)$$

Inserting the initial boundary condition

$$C_{Red}(x,0) = C^*_{Red} \qquad (3)$$

into the image equation gives

$$s\left\{\bar{C}_{Red}(x,s)\right\} - C^*_{Red} = D_{Red}\left\{\frac{\partial^2 \bar{C}_{Red}(x,s)}{\partial x^2}\right\} . \qquad (9)$$

Rearranging, we have

$$\frac{\partial^2 \bar{C}_{Red}(x,s)}{\partial x^2} - \frac{s}{D_{Red}}\left\{\bar{C}_{Red}(x,s)\right\} = \frac{-C^*_{Red}}{D_{Red}} \qquad (10)$$

which is an ordinary differential equation (no longer a partial differential equation). The general solution of Eqn. (10) is given by

$$\overline{C}_{Red}(x,s) = \exp(\alpha x) \tag{11}$$

where

$$\alpha = \pm \left(\frac{s}{D_{Red}}\right)^{1/2} . \tag{12}$$

Therefore,

$$\overline{C}_{Red}(x,s) = A \exp(\alpha x) + B \exp(-\alpha x) + \text{constant}. \tag{13}$$

The constant is determined using a variation of parameter technique [56] which utilizes the two linear equations:

$$V_1'U_1 + V_2'U_2 = 0 \tag{14}$$

and

$$V_1'U_1' + V_2'U_2' = H, \tag{15}$$

where prime denotes the first derivative. Substituting

$$U_1 = \exp(\alpha x) \tag{16}$$

and

$$U_2 = \exp(-\alpha x) \tag{17}$$

results in

$$V_1' \exp(\alpha x) + V_2' \exp(-\alpha x) = 0 \tag{18}$$

and

$$V_1' \alpha \exp(\alpha x) + V_2' (-\alpha) \exp(-\alpha x) = \frac{- C^*_{Red}}{D_{Red}} . \tag{19}$$

By Cramer's rule:

$$V_1' = \frac{\begin{vmatrix} 0 & U_2 \\ H & U_2' \end{vmatrix}}{\begin{vmatrix} U_1 & U_2 \\ U_1' & U_2' \end{vmatrix}} = \frac{\begin{vmatrix} 0 & \exp(-\alpha x) \\ \frac{- C^*_{Red}}{D_{Red}} & -\alpha \exp(-\alpha x) \end{vmatrix}}{\begin{vmatrix} \exp(\alpha x) & \exp(-\alpha x) \\ \alpha \exp(\alpha x) & -\alpha \exp(-\alpha x) \end{vmatrix}} = \frac{-C^*_{Red} \exp(-\alpha x)}{2 (sD_{Red})^{1/2}} \tag{20}$$

and

$$V_2' = \frac{\begin{vmatrix} U_1 & 0 \\ U_1' & H \end{vmatrix}}{\begin{vmatrix} U_1 & U_2 \\ U_1' & U_2' \end{vmatrix}} = \frac{\begin{vmatrix} \exp(\alpha x) & 0 \\ -\alpha \exp(\alpha x) & \frac{-C^*_{Red}}{D_{Red}} \end{vmatrix}}{\begin{vmatrix} \exp(\alpha x) & \exp(-\alpha x) \\ \alpha \exp(\alpha x) & -\alpha \exp(-\alpha x) \end{vmatrix}} = \frac{C^*_{Red} \exp(\alpha x)}{2\ (sD_{Red})^{1/2}} \qquad (21)$$

Now

$$V_1 = \int V_1'\, dx = \int \frac{-C^*_{Red}\ \exp(-\alpha x)dx}{2\ (sD_{Red})^{1/2}} = \left[\frac{-C^*_{Red}(\frac{-1}{\alpha})}{2\ (sD_{Red})^{1/2}}\right.$$

$$\left.\int -\alpha \exp(-\alpha x)dx\right] = \frac{C^*_{Red}\ \exp(-\alpha x)}{2\ \alpha(sD_{Red})^{1/2}} + C_{\cdot 1} \qquad (22)$$

Substituting

$$\alpha = \left(\frac{s}{D_{Red}}\right)^{1/2} \qquad (23)$$

simplifies V_1 to

$$\frac{C^*_{Red}\ \exp\{-x(\frac{s}{D_{Red}})^{1/2}\}}{2\ s} + C_1. \qquad (24)$$

Similarly,

$$V_2 = \int V_2'\, dx = \int \frac{C^*_{Red}\ \exp(\alpha x)dx}{2\ (sD_{Red})^{1/2}} = \left[\frac{C^*_{Red}(\frac{1}{\alpha})}{2\ (sD_{Red})^{1/2}}\right.$$

$$\int \alpha \exp(\alpha x)dx] = \frac{C^{*}_{Red} \exp(\alpha x)}{2\ (sD_{Red})^{1/2}} + C_2 \qquad (25)$$

again substituting

$$\alpha = (\frac{s}{D_{Red}})^{1/2} \qquad (23)$$

results in

$$V_2 = \frac{C^{*}_{Red} \exp\{x\ (\frac{s}{D_{Red}})^{1/2}\}}{2\ s} + C_2. \qquad (26)$$

Therefore,

$$\overline{C}_{Red}(x,s) = V_1U_1 + V_2U_2 = ([\frac{C^{*}_{Red} \exp\{-x(\frac{s}{D_{Red}})^{1/2}\}}{2\ s} + C_1\ ]$$

$$\exp\{x(\frac{s}{D_{Red}})^{1/2}\}) + ([\frac{C^{*}_{Red} \exp\{x(\frac{s}{D_{Red}})^{1/2}\}}{2\ s} + C_2\ ]$$

$$\exp\{-x(\frac{s}{D_{Red}})^{1/2}\}). \qquad (27)$$

Transforming the semi-infinite boundary condition, we have

$$L\ \{\lim_{x\to\infty} C_{Red}(x,t)\} = \lim_{x\to\infty} \{L[C_{Red}(x,t)]\}$$

$$= \lim_{x \to \infty} \bar{C}_{Red}(x,s) = \frac{C^*_{Red}}{s} . \qquad (28)$$

Therefore, A = 0 and

$$\bar{C}_{Red}(x,s) = \frac{C^*_{Red}}{s} + B \exp\{-x(\frac{s}{D_{Red}})^{1/2}\} \qquad (29)$$

Applying the last condition (the surface boundary condition),

$$C_{Red}(0,t) = 0 \text{ for } t > 0 \qquad (5)$$

and taking the Laplace transform

$$L\{C_{Red}(0,t)\} = 0 , \qquad (30)$$

gives

$$\bar{C}_{Red}(0,s) = 0. \qquad (31)$$

Therefore,

$$\bar{C}_{Red}(0,s) = \frac{C^*_{Red}}{s} + B \exp\{0(\frac{s}{D_{Red}})^{1/2}\} = 0 \qquad (32)$$

or

$$B = \frac{- C^{*}_{Red}}{s} \tag{33}$$

Substitution of Eqn. (33) into Eqn. (29) gives the solution

$$\bar{C}_{Red}(x,s) = \frac{C^{*}_{Red}}{s} \left[1 - \exp\left\{-x\left(\frac{s}{D_{Red}}\right)^{1/2}\right\}\right] . \tag{34}$$

In the absence of convection and migration, the flux is

$$- J(0,t) = \frac{i(t)}{nFA} = D_{Red}\left[\frac{\partial C_{Red}(x,t)}{\partial x}\right]_{x=0} \tag{35}$$

at the electrode surface (x = 0). This transforms to

$$\frac{i(s)}{nFA} = D_{Red}\left[\frac{\partial \bar{C}_{Red}(x,s)}{\partial x}\right]_{x=0} \tag{36}$$

where n, F, and A represent the number of electrons occurring in the electron transfer, the Faraday constant, and the area of the electrode surface, respectively. Substituting Eqn. (34) for $\bar{C}_{Red}(x,s)$ results in:

$$i(s) = nFAD_{Red}\left\{\frac{\partial\left[\frac{C^{*}_{Red}}{s} - \frac{C^{*}_{Red}}{s}\exp\left\{-x\left(\frac{s}{D_{Red}}\right)^{1/2}\right\}\right.}{\partial x}\right\}_{x=0} \tag{37}$$

or

$$i(s) = nFAD_{Red} \left\{ \left(\frac{s}{D_{Red}}\right)^{1/2} \frac{C^*_{Red}}{s} \exp\left[-x\left(\frac{s}{D_{Red}}\right)^{1/2}\right] \right\}_{x=0} \quad (38)$$

and for x = 0 we have

$$i(s) = \frac{nFAD_{Red}^{1/2} C^*_{Red}}{s^{1/2}}. \quad (39)$$

Using the fact that

$$L^{-1}\left(\frac{1}{s^{1/2}}\right) = \frac{1}{(\pi t)^{1/2}}, \quad (40)$$

and taking the inverse Laplace transform of i(s) results in:

$$i(t) = \frac{nFAD_{Red}^{1/2} C^*_{Red}}{(\pi t)^{1/2}}, \quad (41)$$

which is the familiar Cottrell equation. Since, [18]

$$A(t) = \varepsilon \int_0^t C_{O_x} dx = \varepsilon \int_0^t \frac{i(t)dt}{nFA} \quad (42)$$

where ε is the molar absorptivity of the absorbing species, and substituting equation 41 for i(t) results in

$$A(t) = \varepsilon_0 \int^t \frac{D_{Red}^{1/2} C^*_{Red} dt}{(\pi t)^{1/2}} \quad (43)$$

therefore,

$$A(t) = \frac{2\ \varepsilon\ D_{Red}^{1/2}\ \ C_{Red}^{*}\ t^{1/2}}{\pi^{1/2}}. \qquad (44)$$

Now, if R_1 is equivalent to the reflected light intensity during the potential step and R_0 is equivalent to that before the potential step then

$$\frac{\Delta R}{R} \equiv \frac{R_1 - R_0}{R_0} \qquad (45)$$

and

$$1 + \frac{\Delta R}{R} = 1 + \frac{R_1 - R_0}{R_0} = \frac{R_1}{R_0} \qquad (46)$$

From Beer's law

$$A(t) = -\log\left(\frac{R_1}{R_0}\right) = \frac{-1}{2.303}\ \ln\left(\frac{R_1}{R_0}\right) \qquad (47)$$

and substituting for R_1/R_0 gives:

$$A(t) = \frac{-1}{2.303}\ \ln\left(1 + \frac{\Delta R}{R}\right)\ . \qquad (48)$$

A Taylor's series expension of the natural logarithm yields

$$\ln\left(1 + \frac{\Delta R}{R}\right) = \frac{\Delta R}{R} - \frac{\left(\frac{\Delta R}{R}\right)^2}{2} + \ldots \qquad (49)$$

So for small $\Delta R/R$,

$$\ln\left(1 + \frac{\Delta R}{R}\right) \cong \frac{\Delta R}{R} , \tag{50}$$

which after substitution into Eqn. (48) yields

$$A(t) = \frac{-1}{2.303}\left(\frac{\Delta R}{R}\right) . \tag{51}$$

Therefore,

$$\frac{\Delta R}{R} = -2.303\ A(t) = \frac{-2.303\left(2\ \varepsilon\ D_{Red}^{1/2}\ C_{Red}^{*}\ t^{1/2}\right)}{\pi^{1/2}} \tag{52}$$

or

$$\frac{\Delta R}{R} = \frac{-4.606\ \varepsilon\ D_{0}^{1/2}\ C_{Red}^{*}\ t^{1/2}}{\pi^{1/2}} \tag{53}$$

The special light path geometry of the cell used must be considered. We note that the beam of light passes through the solution and diffusion layer twice (Figure 2). For an angle σ taken with respect to a normal to the surface of the electrode, the pathlength is $q = 2x/\cos\sigma$. Substituting $\Delta\varepsilon = \varepsilon_2 - \varepsilon_1$ for ε in the case of both O_x and Red being absorbing species with different molar absorptivities, ε_2 and ε_1, we have the final result:

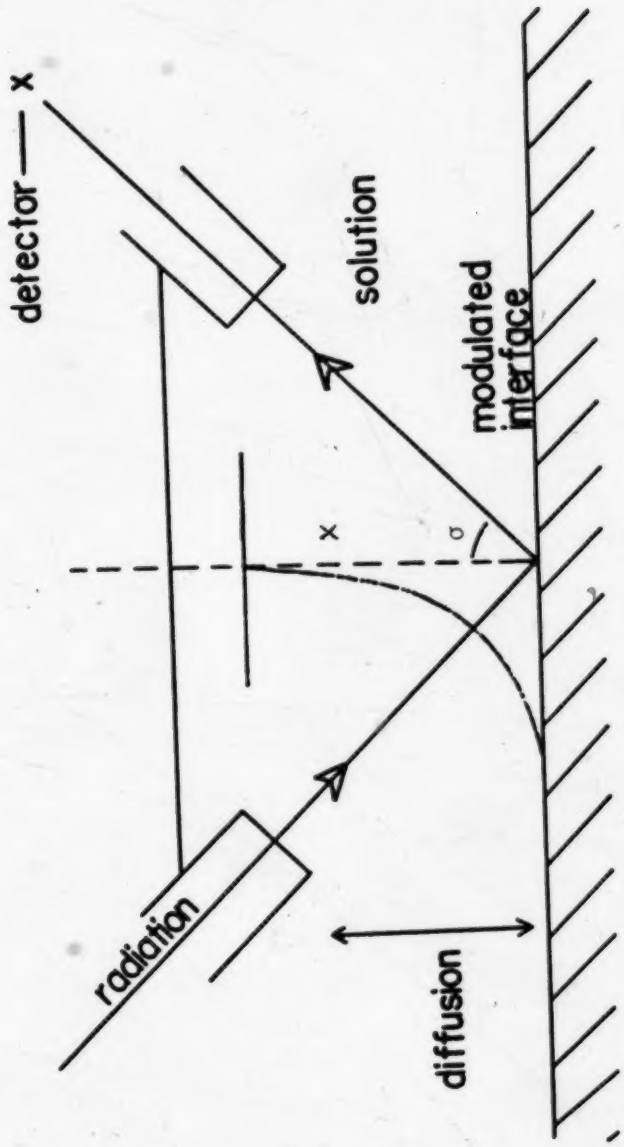

Figure 2. Light path geometry of reflectance cell.

$$\frac{\Delta R}{R} = \frac{-9.212\ \Delta\varepsilon\ D_{Red}^{1/2}\ C_{Red}^{*}\ t^{1/2}}{\pi^{1/2}\ \cos\ \sigma} \qquad (54)$$

CHAPTER 3

EXPERIMENTAL

3.1 Preparations and Purifications

3.1.1 Purification of Acetonitrile

The electrochemical solvent used in this work was acetonitrile. Purification of acetonitrile was carried out using a modification of the procedure given by Mann *et al.* [57]. Due to the electrochemical activity of the impurities usually present in commercial grade acetonitrile, they must be removed before the solvent can be used. The impurities may include unsaturated nitriles, acetamide, ammonium acetate, acetic acid, aldehydes, amines, ammonia, and water.

Approximately 2.5 L of commercial grade acetonitrile was rapidly distilled using a short Vigreux column in order to remove a large percentage of the impurities present. This greatly reduces the risk of a fire or explosion in the subsequent oxidative purification to be carried out. The first and last 100 mL were discarded, and the center 2.3 L were collected and stored over 10 g of calcium hydride for at least 24 h. No more than 0.2%

water can be present in the next step in order for the successful removal of aromatic hydrocarbons to be accomplished. The solvent was decanted and 25 mL of benzoyl chloride were added and the mixture was refluxed for one hour. The solvent was then distilled (5 mL/m) and collected in a flask containing 25 mL of water which was necessary to hydrolyze any benzoyl chloride carried over. The last 100 mL of solvent to be distilled were discarded. The solvent was redistilled discarding the first 50 mL and last 100 mL. 25 g of potassium permanganate were added to the distillate and this solution was rapidly distilled discarding the first and last 50 mL of distillate. A drying tube was used to keep atmospheric water out. Any ammonia present was then neutralized with concentrated sulfuric acid whereupon the acidic acetonitrile was then decanted from any ammonium sulfate that had precipitated. The solvent was then distilled again (10 mL/m), this time discarding the first and last 50 mL and collecting the distillate over 25 g of calcium hydride. The distillate containing the calcium hydride was then distilled (1 mL/m) in a carefully dried distillation apparatus which contained a four foot insulated column packed with glass helices. The distillation was carried out under a dry argon atmosphere and the first 50 mL and last 100 mL were discarded. The

final distillate, purified acetonitrile, was stored over Woelm super grade alumina under a dry argon atmosphere until needed.

This modified purification procedure gave a 65% yield relative to the starting material. The purified solvent gave, on the average, a transmittance of better than 90% at 200 nm. Using tetra-n-butylammonium tetrafluoroborate as supporting electrolyte (0.1 M), the steady-state background current at +3.00 V versus a Ag/Ag^+ (0.01 M) electrode was less than 50 $\mu A/cm^2$. This background current is only achievable if the glassware used is scrupulously dried. The usual procedure is to use Woelm super grade alumina in the electrochemical cell to remove any last traces of water.

Caledon HPLC grade acetonitrile with 0.006% water could also be used after drying over Woelm super grade alumina overnight without further purification. The product is, however, very costly.

3.2 Supporting Electrolyes

3.2.1 Preparation of Tetra-n-butylammonium Tetrafluoroborate

Tetra-n-butylammonium tetrafluoroborate was prepared by a modified version of the procedure used by Lund and Iverson [58]. 340 g of tetra-n-butylammonium hydrogen

sulfate was dissolved in the minimum amount of water necessary and filtered. To the tetra-n-butylammonium hydrogen sulfate solution was added slowly and with stirring a solution of 100 g of sodium tetrafluoroborate. The immediately precipitated tetra-n-butylammonium tetrafluoroborate was filtered and washed with two 100 mL portions of ice cold distilled water. The precipitate was then dissolved in approximately 75 mL of methylene chloride and transferred to a separatory funnel and shaken. The lower layer containing methylene chloride and tetra-n-butylammonium tetrafluoroborate was added to 300 mL of cold diethyl ether with vigorous stirring. The upper layer containing water and sodium bisulfate was discarded. The tetra-n-butylammonium tetrafluoroborate in the diethyl ether solution, after slowly precipitating, was filtered in 15 minutes. The precipitate was then redissolved in methylene chloride and reprecipitated upon addition of cold diethyl ether. This was performed a total of three times before the final precipitate, after being filtered, was dried under vacuum at 40°C for at least 72 hours. The yield was 75% with respect to the tetra-n-butylammonium hydrogen sulfate.

3.2.2 Purification of Lithium Perchlorate

Lithium perchlorate (Thiokol) was purified with two recrystallizations from triply distilled water and was then dried at 100°C under vacuum overnight [59].

3.3 Commercial Chemicals

1,4-Dimethoxy-9,10-diphenylanthracene (Aldrich 99.9%) was used as received.

2,6-Di-tert-butyl-4-(4-methoxyphenyl)-aniline was used as received.

3.4 Optical Reflectance Cell and Electrodes

The optical working electrode used was a thin platinum cylinder (2 mm × 6 mm diameter) which had been silver soldered onto the end of a longer solid brass cylinder (6 mm × 160 mm) (Figure 3). With a portion of the brass cylinder coated with epoxy, approximately one-half of the brass cylinder (the half containing the platinum disk) was then shrink-fitted into a 3 mm thick hollow Kel-F cylinder such that only the platinum surface remained exposed. The resulting seal was resistant to organic solvents. The remaining half of the brass cylinder was fitted with a Kel-F cylinder which was loose enough to be removed at will. A rubber O-ring was inserted between the stationary and removable Kel-F cylinders such that when a brass nut was tightened on the end of the brass cylinder containing screw threads, the movable Kel-F cylinder would squeeze and expand the O-

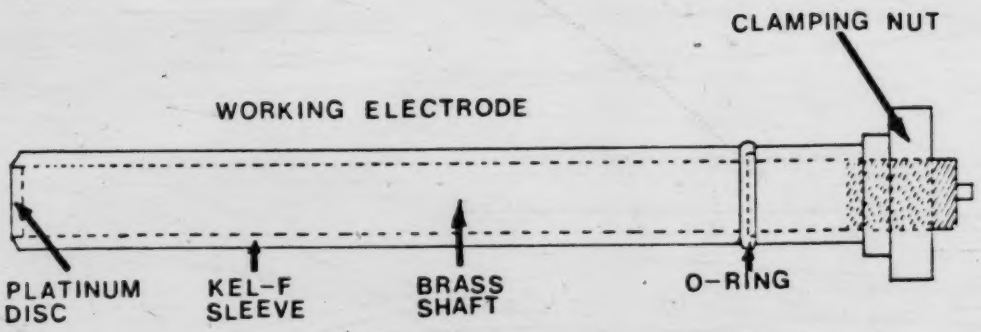

Figure 3. Optical working electrode.

ring. The entire Kel-F sleeved brass cylinder fit into a syringe barrel opening in the optical reflectance cell with a small enough clearance (0.1 to 0.2 mm) such that if the brass nut were tightened the O-ring would form a seal between this working electrode and the inner wall of the syringe barrel opening.

The platinum surface of the working electrode was polished by mounting it in an aluminum mandril (Figure 4) which was used to keep the plane of the electrode surface perpendicular to the electrode's brass cylinder shaft. After securing the electrode with the two screws available, it was polished using increasingly finer grains (1.0 μm, 0.05 μm, 0.03 μm) of polishing alumina (Baikalox) on a polishing pad (Buchler) which had been stretched and secured to an 8 inch square piece of plate glass. The successive polishings were performed with the use of distilled water. It was possible to obtain reproducible mirror flat surfaces with this procedure. Before using the electrode, it was cleaned with acetone, sulfuric acid, and distilled water.

The secondary electrode used consisted of a thin platinum disk attached to a platinum wire which was sealed into the end of a glass joint that fit into its counter port opening located opposite the working electrode.

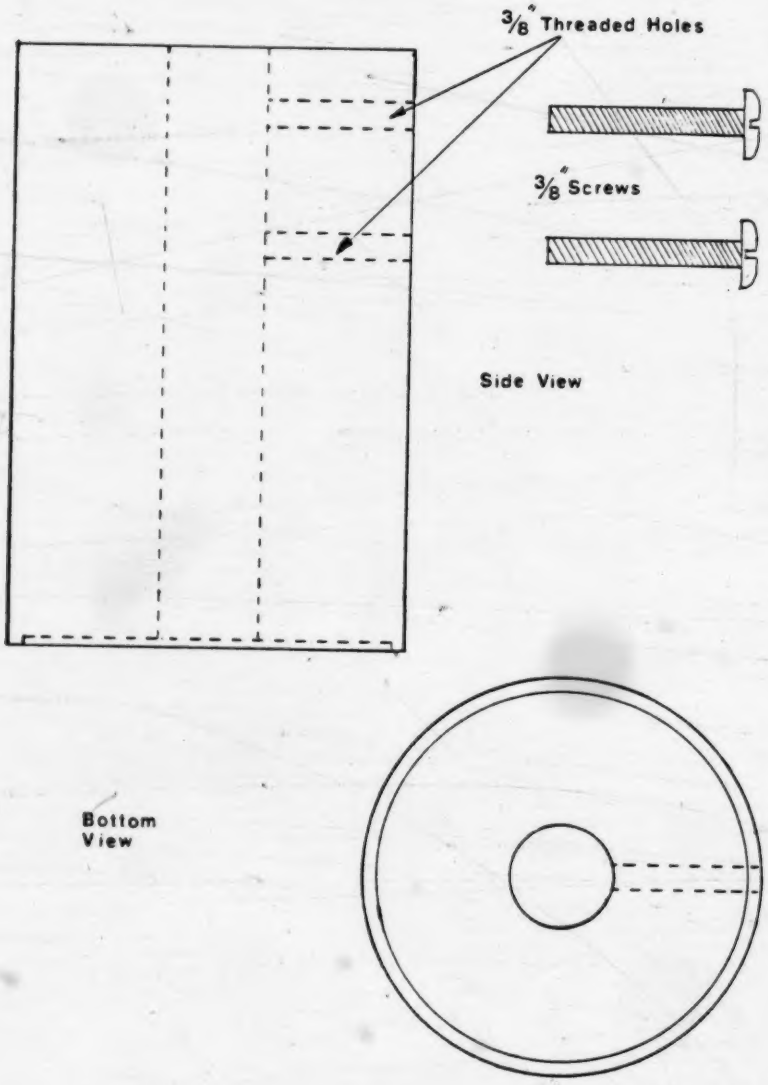

Figure 4. Polishing mandril for the optical working electrode.

The Ag/Ag^+ reference electrode used was isolated from the rest of the cell via a Luggin capillary containing a glass stopcock. The loosely fitting stopcock was wetted before being closed. The Luggin capillary led to a Ag/Ag^+ reference electrode. This section was inserted into a second syringe barrel opening located such that the tip of the Luggin capillary could be positioned close to the working electrode surface without interfering with the optical path. The distance of approach was adjusted so as to be the minimum achievable without driving the potentiostat into oscillation. The Luggin capillary was held in position via a movable O-ring on the capillary itself which would not fit into the syringe barrel opening. The Ag/Ag^+ reference electrode was itself isolated from the Luggin chamber via a glass frit.

The optical reflectance cell is shown in Figure 5. The platinum working electrode is positioned such that the incident light which has passed in through the first of two quartz windows will pass out through the second quartz window after reflection from the electrode surface. The secondary electrode is approximately 3 cm opposite the working electrode surface.

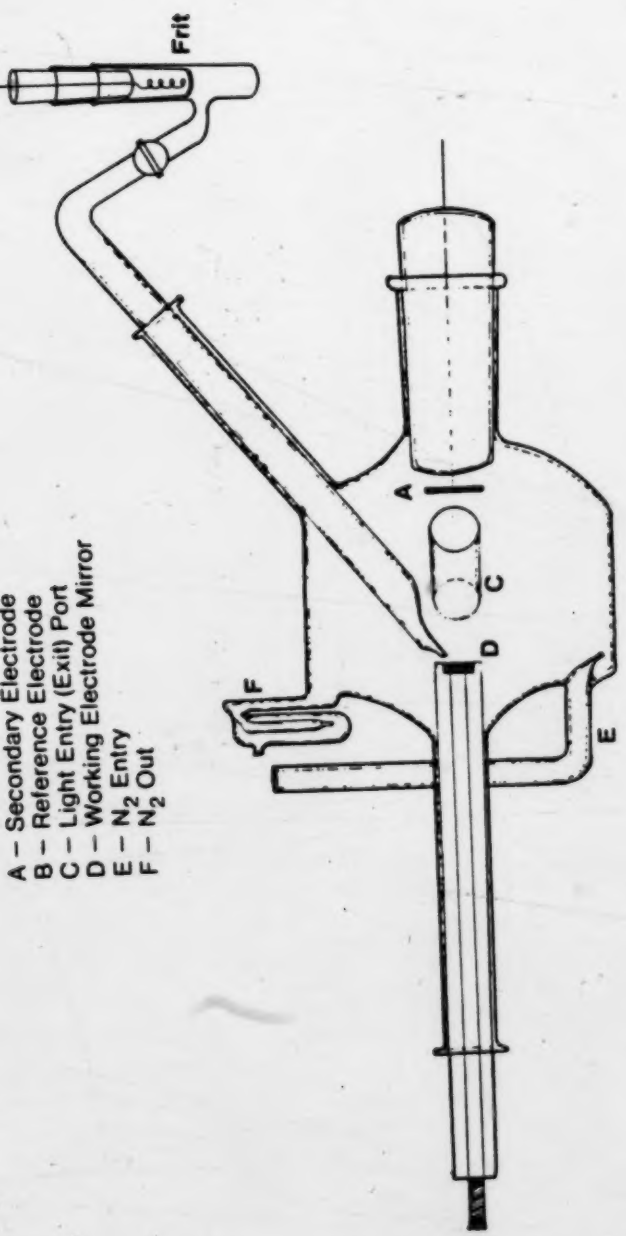

Figure 5. **Optical Cell Used For Modulated Reflectance Experiments**

3.5 Experimental Apparatus

The experimental apparatus used to carry out the spectrophotometric equivalent of chronoamperometry is illustrated in Figure 6. The components used to perform the electrochemistry consist of a Hi-Tek Instruments PPR1 waveform generator and a Hi-Tek DT2101 potentiostat. The components utilized to obtain the optical signal consist of: a 35 watt quartz-halogen lamp, two 75 mm focal length lenses, the straight slit (Model No. 14115) and housing of a Spex Industries monochromator (Model No. 1401) along with the accompanying John-Yvon grating (1221 g/mm blazed at 5000 Å), and a Fairchild CCD 133. The components used to process the optically generated signals include an AIM 65/6502 microprocessor and an Analog Devices 14 bit high speed ADC 1131k. In order to perform the chronoamperometric experiments, it was necessary first to record cyclic voltammograms of the compound of interest. This was done in order to determine the initial potential and the magnitude of the potential step necessary to arrive at a potential well into the diffusion limited region of the experiment. The cyclic voltammograms were obtained at a sweep rate of 100 mV/s using the same solutions and optical reflectance cell as were used with the chronoamperometric experiments. The potentiostat and waveform generator were also the same as used in the

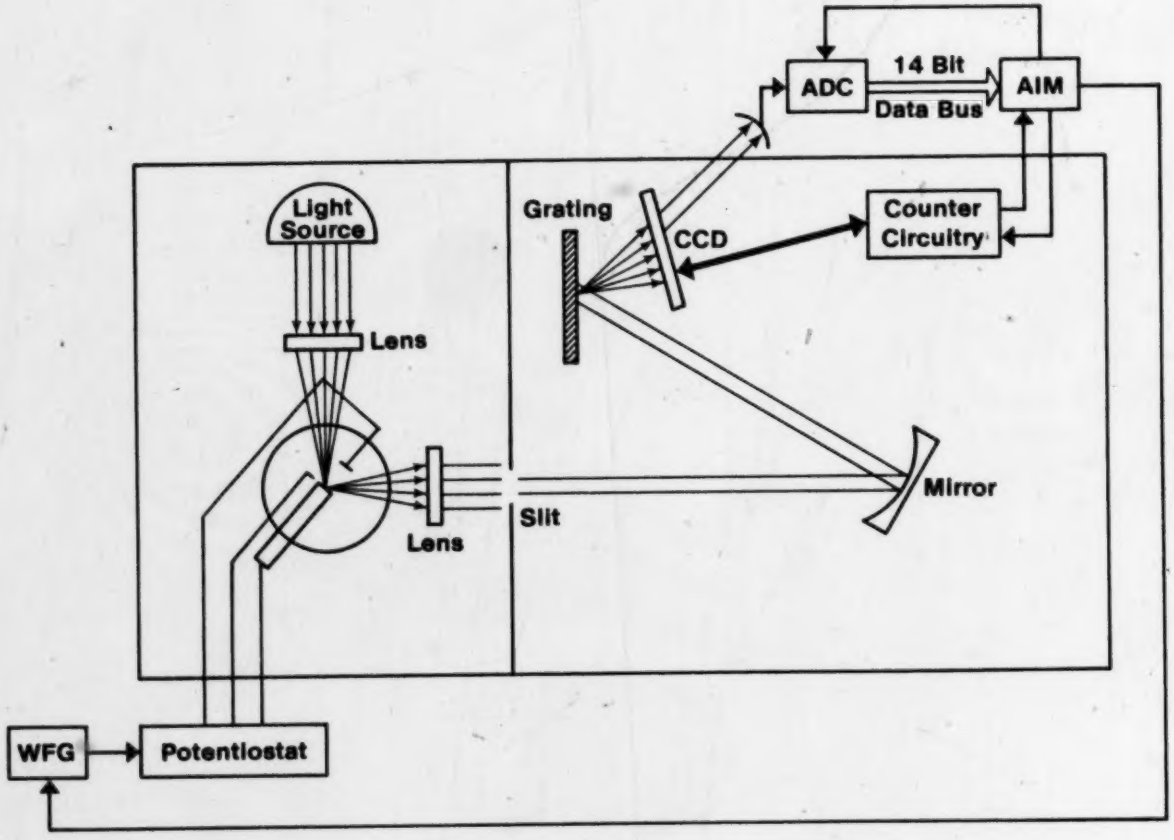

Figure 6. Experimental apparatus used to perform reflectance experiments with a CCD.

chronoamperometric experiments with the cyclic voltammograms recorded on a Gould HR2000 storage recorder.

A general overview of the electronics utilized to control and interface the CCD to an AIM 65/6502 microprocessor during a chronoamperometric experiment will now be given, followed by a section containing a more detailed description with the appropriate timing diagrams.

The CCD used in this research contained one-thousand twenty-four individual photoelements and is described in Section 3.6. It required two synchronized clock signals for proper operation. The first was a sixteen kilohertz integration signal generated by a voltage controlled oscillator (VCO) (Figure 7). The other was a ten megahertz data signal generated by a twenty megahertz crystal clock oscillator (CCO) whose frequency was halved by passing it through a D-type flip flop (FF1). A D-type flip flop is an electronic clocked logic device that presents the D input signal level to the Q output whenever the clock input undergoes a positive transition [60] (a change in voltage from low to high). The sixteen kilohertz integration signal was used to enable a second D-type flip flop (FF2) which receives its D input values from the output of the first flip flop (FF1). This resulted in the properly synchronized clock signals (Figure 8) which allowed the CCD to operate at a "free

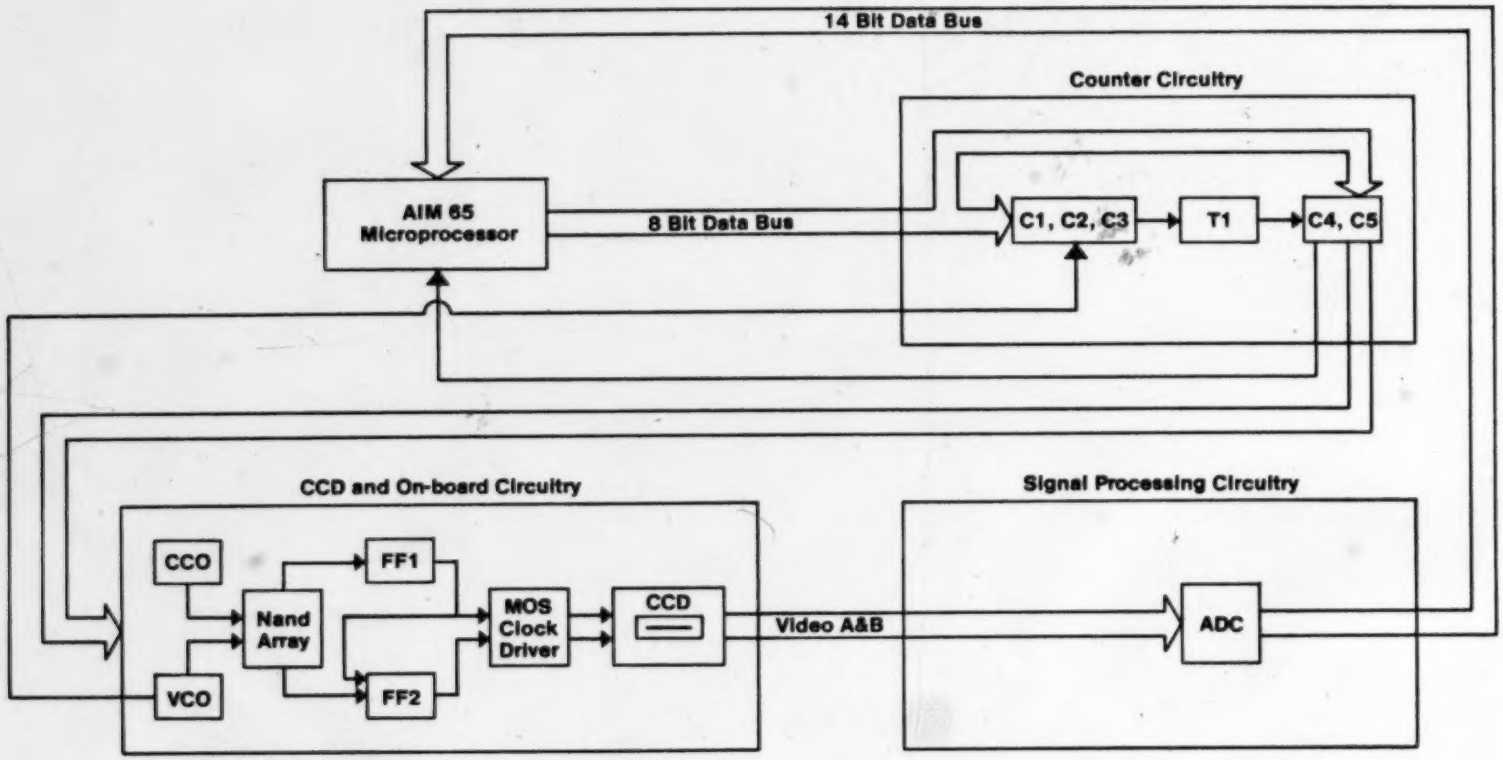

Figure 7. Block diagram of electronic system.

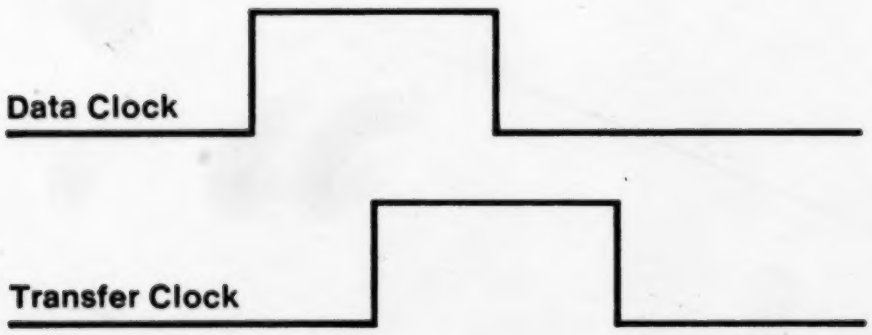

Figure 8. Synchronized clock signals.

running" rate of sixteen kilohertz with approximately sixty microseconds being equal to one integration period. The sixteen kilohertz integration signal was also used to clock the first of three parallel decade counters (C1, C2, C3). These decade counters determined the amount of time between the initiation of the potential step and the beginning of the integration period by counting a specified number of the positive transitions occurring in the integration signal. This delay time was adjustable under software control via the microprocessor, from zero to sixty milliseconds in sixty microsecond increments. The integration period was terminated by the second of two separate parallel decade counters (C4, C5). These counters were clocked by a 555 timer (T1) which ran astably at eighteen kilohertz, allowing the integration period to vary from fifty-five microseconds to five milliseconds, programmable in fifty-five microsecond increments. After the integration period was terminated the microprocessor serially clocked out the CCD shift registers containing the analog equivalents of the incident light that had interacted with the photoelements. These were converted from analog to digital signals with a fourteen bit analog-to-digital converter (ADC) and were stored in the microprocessor. The microprocessor signal averaged a previously programmed

number of scans by summing and storing the spectra, with the spectrum of an electrogenerated species and the background spectrum taken in alternation.

With the previous general overview in mind, the detailed operation of the entire electronic system during an experiment will be given below. In order to facilitate the understanding of the circuitry, the electronic system has been divided into four main parts and itemized below, each with a list of the important components contained therein.

1. The AIM 65/6502 microprocessor. The microprocessor provided:
   a. a waveform generator (WFG) control line.
   b. a counter circuitry reset line.
   c. a CCD selector line.
   d. a three bit load control bus.
   e. an eight bit data bus.
   f. a separate fourteen bit data bus.
   g. an AIM data clock line.
   h. an interrupt request line.
2. The CCD and on-board circuitry (Figure 9). This consisted of:
   a. the CCD.
   b. one dual D-type (high speed) flip flop (FF). (Dual meaning there are two independently operating D-type FF's per package.)

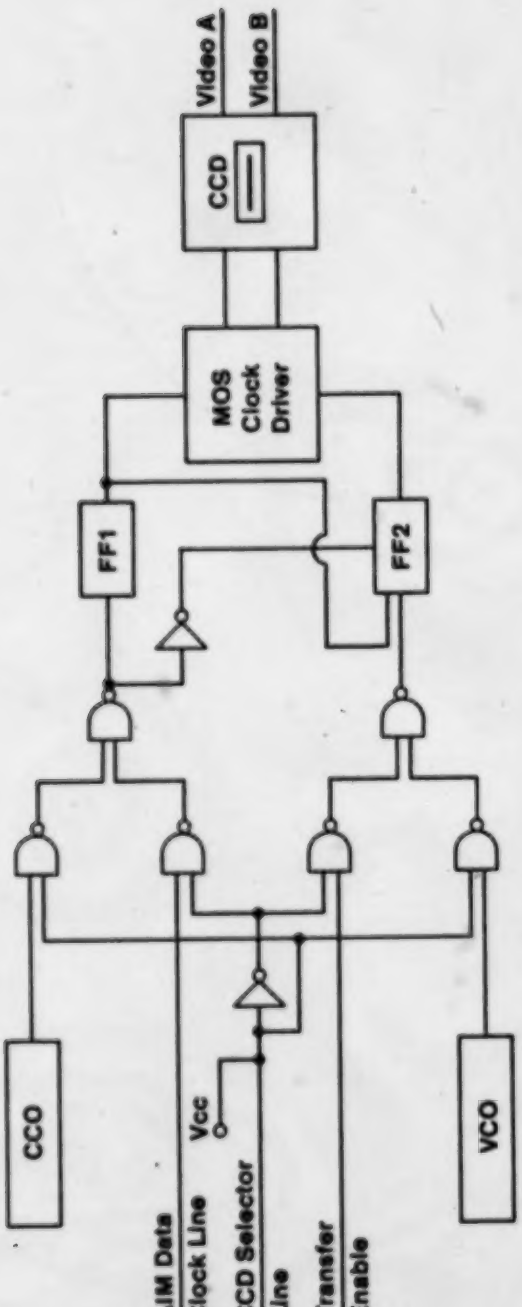

Figure 9. CCD and on-board circuitry.

c. one voltage controlled oscillator (VCO) set to run at a frequency of sixteen kilohertz.

d. one-twenty megahertz crystal clock oscillator (CCO).

e. two quad two-input nand gates. A nand gate is a logic device whose output is high whenever any one or both of the inputs are low. If both inputs are high, its output is low [60]. A quad two-input nand gate is a package containing four independent nand gates, each with two inputs.

f. one dual MOS clock driver. This was a driver used to amplify a low amplitude input clock signal to a higher amplitude (as required by the CCD).

3. The counter circuitry (Figure 10). This consisted of:

a. five decade counters.

b. three dual D-type FF's.

c. two 555 timers (astable mode). These timers provided preset frequency signals.

d. three quad two-input nand gates.

4. The signal processing circuitry (Figure 11). This consisted of:

a. two voltage followers.

b. one summing amplifier.

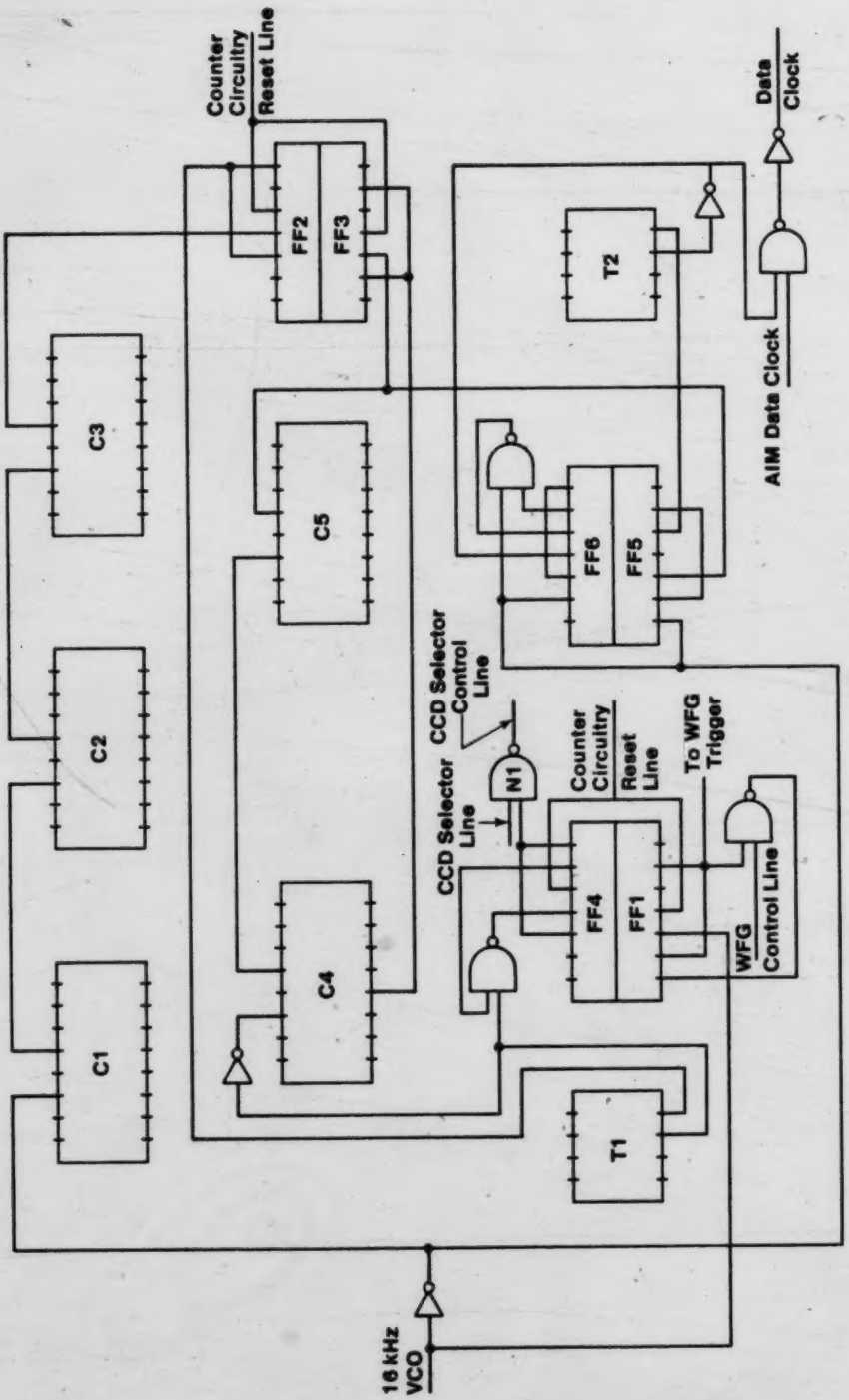

Figure 10. Counter circuitry.

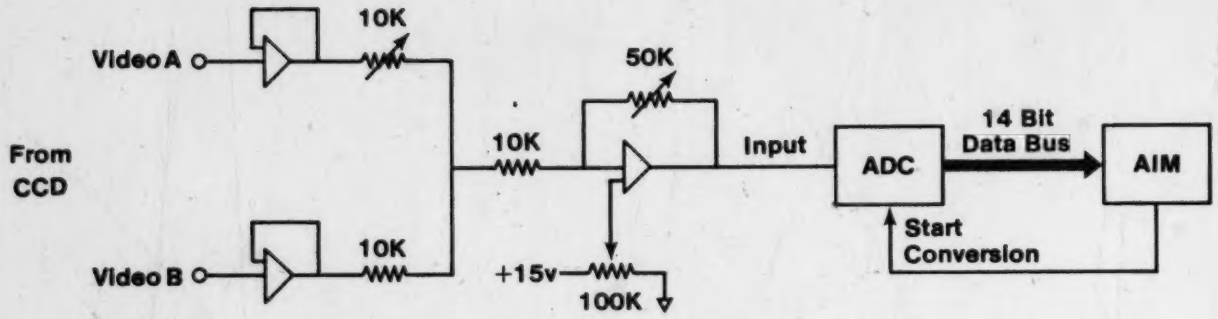

Figure 11. Signal processing circuitry.

c. one fourteen bit analog-to-digital converter (ADC).

The system was ready to run under microprocessor control (see Appendix A for program) after the following preliminary operations were carried out:

1. The desired potential pulse duration and magnitude were set on the waveform generator along with any accompanying settings on the potentiostat.

2. The following time periods were entered into the microprocessor:
   a. the delay between the onset of the potential pulse and the start of the light integration period.
   b. the duration of the light integration period.
   c. the time interval between potential pulses necessary to allow the electrochemical system to relax back to its original conditions.

3. The number of repetitions (scans) to be averaged was entered into the microprocessor.

4. The optical reflectance cell was aligned.

5. The light source was on and the slit width to the monochromator was adjusted.

6. The potentiostat was manually enabled.

To begin the experiment, one of the three available function keys (F1) on the microprocessor was depressed causing the microprocessor to immediately jump to the beginning of the software program and start execution. The microprocessor took the CCD selector line high by bringing low one of the inputs to nand gate N1 (Figure 10) which was located in the counter circuitry. This enabling of the on-board sixteen kilohertz VCO and twenty megahertz CCO (Figure 9), via an array of nand gates, allowed the CCD to "free run", taking spectra at sixty microseconds per scan. Next, the counter circuitry was enabled (this will be explained later) as the WFG control line was simultaneously brought high. At this point, the counter circuitry had no control over the CCD, but the WFG was triggered (only once) due to the indeterminate state of FF1 upon start-up. After a maximum of sixty milliseconds the counter circuitry disabled itself (also explained later) and signaled the microprocessor that it had done so, via the interrupt request line. In the meantime, the microprocessor had cleared all the memory necessary for data storage (approximately 8K). After waiting the required relaxation time for the electrochemical system (in case the WFG had been triggered), the microprocessor checked to see if the counter circuitry had disabled itself indicating a properly operating counter

circuitry. The counter circuitry was now in a predetermined state (all input and output levels were known). Up to this point the experiment had lasted about four seconds with the four seconds determined by the electrochemical relaxation time.

To aid in explaining the operation of the system, timing diagrams (Figures 12 and 13) will be used. The microprocessor, having been signaled that the counter circuitry had disabled itself, loaded the five decade counters located in the counter circuitry (Figure 14). The first two decade counters loaded under software control, C4 and C5, determine the light integration period. To load them, the microprocessor presented the binary equivalent of the previously entered integration period onto an eight bit data bus (eight separate wires). This eight bit data bus terminates at the load inputs (L1, L2, L4, L8) of the decade counters with the four higher bits connected to the load inputs of decade counters C2 and C5 and the four lower bits connected to decade counters C1, C3, and C4. The microprocessor then selected the proper decade counter to load via a three bit load control bus. When any one of these three bus lines were brought from a low to a high level the data on the data bus was loaded into the corresponding decade counter. The sequence was as follows:

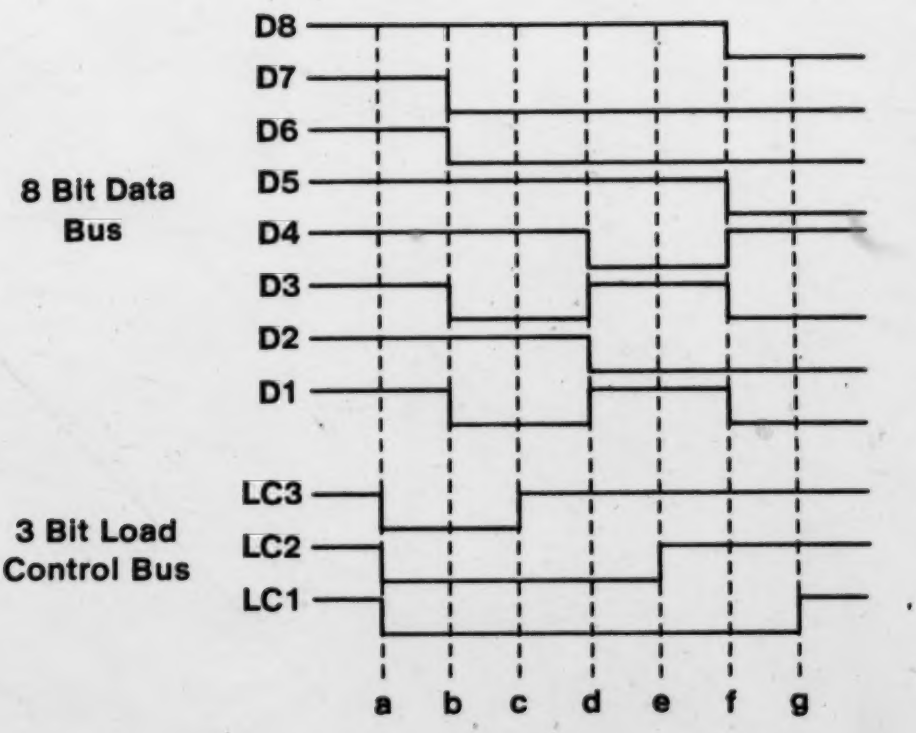

Figure 12. Timing diagram for loading of decade counters.

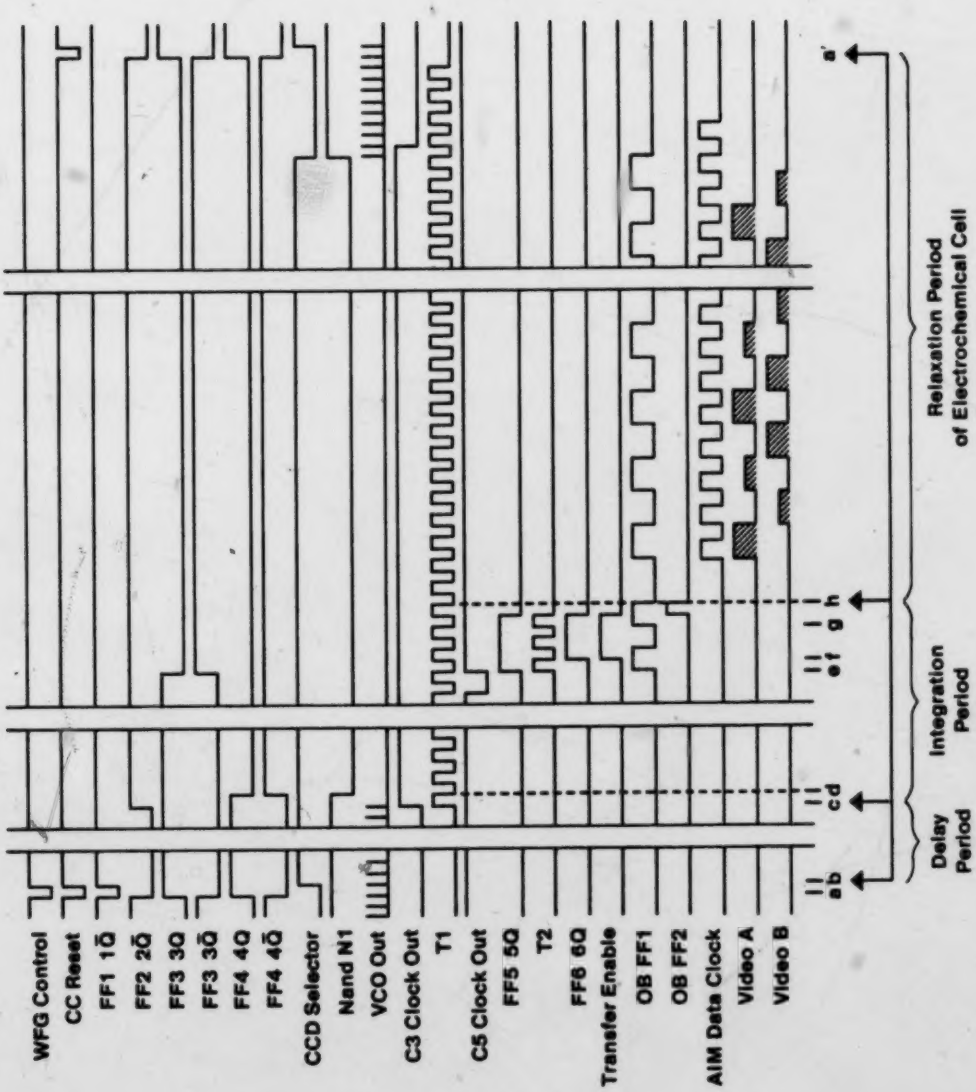

Figure 13. Timing diagram for electronic system operation.

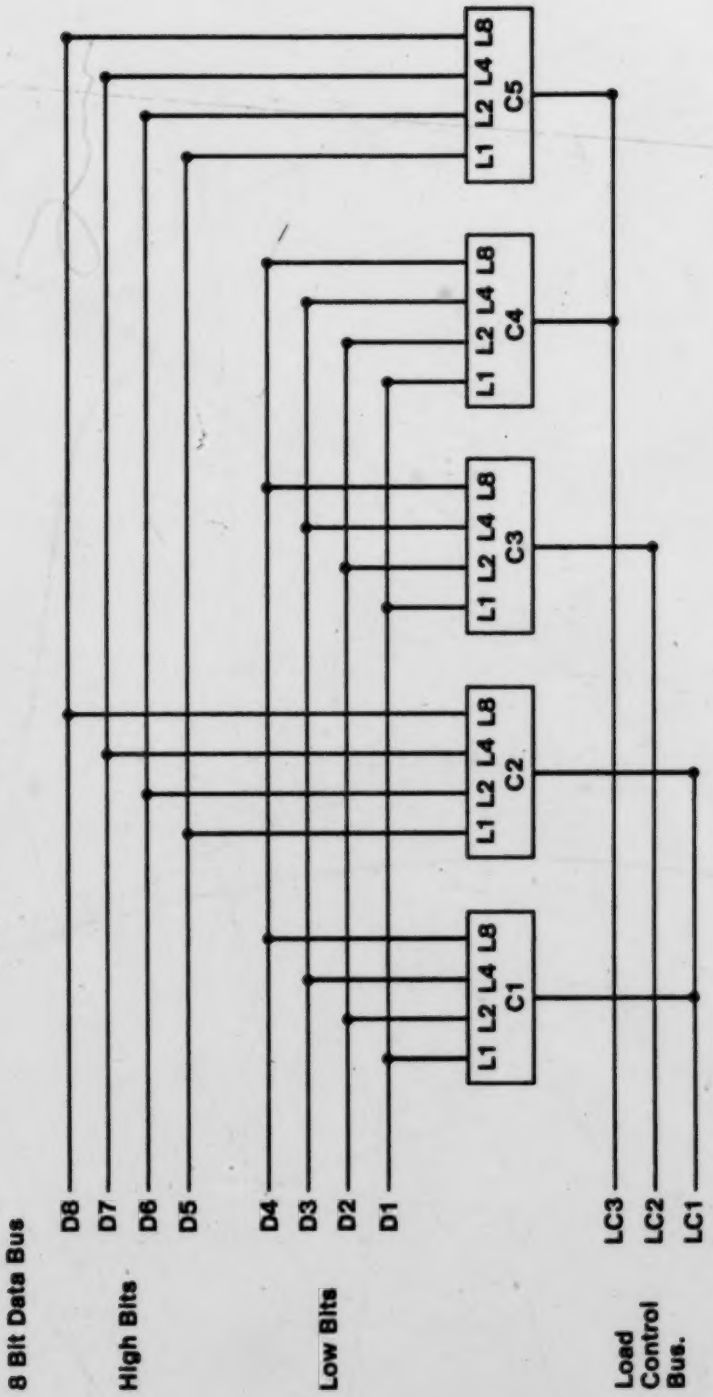

Figure 14. Decade counters.

1. All three load control lines are taken low (Figure 12, pt. a).

2. The binary equivalent of the integration period was placed on the eight bit data bus (Figure 12, pt. b).

3. Load control line three was brought high (Figure 12, pt. c). This loaded the four low bits on the data bus into decade counter C4 and the four higher bits into decade counter C5.

4. The delay time was decoded and part of it (four highest bits) was placed on the four low bits of the data bus (Figure 12, pt. d), followed by load control line two being brought high (Figure 12, pt. e), thus loading decade counter C3.

5. The same sequence as was used for decade counters C4 and C5 was followed for C1 and C2 only using load control line one (Figure 12, pts. f and g).

With all five decade counters loaded, the microprocessor was ready to turn control of the CCD over to the counter circuitry (Figure 10). It did this by pulsing both the WFG control lines and the counter circuitry reset line low (Figure 13, pt. a) then high and also changed the CCD selector line to a high level (Figure 13, pt. b). This caused the WFG trigger to be enabled and

also set FF's 1, 2, 3 and 4. When FF's 2 and 3 are set their $\overline{Q}$ outputs are changed from a high value, previously set by the test run, to a low value which enabled the decade counters. Decade counter C1 then counted the pulses delivered by the sixteen kilohertz VCO which were sixty microseconds apart with the first pulse clocking FF1's $1\overline{Q}$ output high which triggered the WFG. Since decade counters C1, C2, and C3 were cascaded they counted, in sixty microsecond increments, the required number of pulses to arrive at the delay time (Figure 13, pts b to c). Upon finishing, decade counter C3 clocks the $2\overline{Q}$ output on FF2 high (Figure 13, pt. c) which disabled decade counter C1 also disabling C2 and C3. At the same time, the 555 timer T1, wired to run in the astable mode (continuous) at eighteen kilohertz was enabled which started clocking decade counters C4 and C5. The first high to low transition of 555 timer T1, which occurred fifty-five microseconds after it was enabled, clocked FF4's $4\overline{Q}$ output high (Figure 13, pt. d) which along with the CCD selector line was an input to nand gate N1 controlling the CCD selector control line of the on-board circuitry. When $4\overline{Q}$ went high (the CCD selector line was already high), the output of nand gate N1 took the CCD selector control line low which disabled the on-board VCO and CCO five microseconds before the next VCO controlled

transfer pulse would have occurred. Thus, the light integration period started with the last pulse delivered by the sixteen kilohertz VCO (Figure 13, pt. c). Next, decade counters C4 and C5 counted the required number of pulses delivered by T1, to arrive at the light integration period (Figure 13, pt. e) whereupon they disabled themselves by clocking FF3's $3\overline{Q}$ output high. FF5's 5Q output is also clocked high (previously set low by the sixteen kilohertz VCO) which enabled 555 timer T2. This timer clocked FF6's 6Q output high (also previously set low by the sixteen kilohertz VCO) taking the transfer enable line high (Figure 13, pt. f) which was kept high via FF6 and it associated nand gate. The ony time the required transfer pulse can get through to the CCD (other than in the "free running" mode) is when the transfer enable line is high. This now being the case, timer T2 indirectly provided this transfer pulse. It did this by clocking, on its positive transitions, on-board FF1 which provided the inputs to on-board FF2. On-board FF2, which had been enabled by the transfer enable line, was also clocked by timer T2, but on its negative transitions. The result was the properly synchronized transfer and transport signals required by the CCD (Figure 13, pts. g to h) which caused the CCD to simultaneously shift all of the one-thousand and twenty-four photon generated analog

signals out into the two analog shift registers. The transfer pulse was also used to clear the 5Q and 6Q outputs on FF's 5 and 6 to prevent any more transfer pulses from occurring. The counter circuitry, having completed its function, signaled the microprocessor via FF3's 3Q output on the interrupt request line. The microprocessor took over and delivered individual data clock pulses to the on-board circuitry via the AIM data clock line, causing the CCD to serially shift out the analog shift registers alternately to two video lines, A and B (Figure 13, pts. h to i). Each video line was buffered by a voltage follower for protection with both then being summed at a summing amplifier (Figure 11). The summing amplifier also subtracted a constant d.c. bias voltage and amplified the result up to a maximum of ten volts. This signal was fed into a fourteen bit analog-to-digital converter (ADC) which was simultaneously being triggered by the data clock pulses. The resulting digital information was then transported to and stored in the microprocessor via a fourteen bit data bus. The analog-to-digital conversion and subsequent storage of all one-thousand and twenty-four bits of information required approximately twenty milliseconds. The CCD was then allowed to "free run" while the microprocessor summed the recently stored data with any previously stored data. The

rest of the relaxation time was then waited (Figure 13, pts. i to j) and the entire cycle was repeated only this time without enabling the WFG (Figure 13, pt. a'), thus acquiring a background spectrum.

After the required number of spectra had been summed, the two resulting spectra consisting of electrogenerated species and background were serially transferred via an RS232 Asynchronous Communication Interface Adapter to a Three Rivers Corporation Perq computer for processing and plotting, resulting in the spectrum of the electrogenerated species. A hard copy of the resultant spectrum was then obtained using a Bascom-Turner (Model 2120) storage recorder.

3.6 Array Detectors

A brief description of the operational characteristics of a CCD and a PDA are given in this section. These characteristics are then compared and the superiority of the CCD over the PDA is demonstrated.

The central active component of the CCD [61-68] is a MOS (metal-oxide-semiconductor) capacitor [69,70] which consists of a metal electrode and a doped semiconductor separated by an oxide layer (Figure 15). In this work, the semiconductor is a p-type doped silicon substrate. By applying a positive potential to the metal electrode of

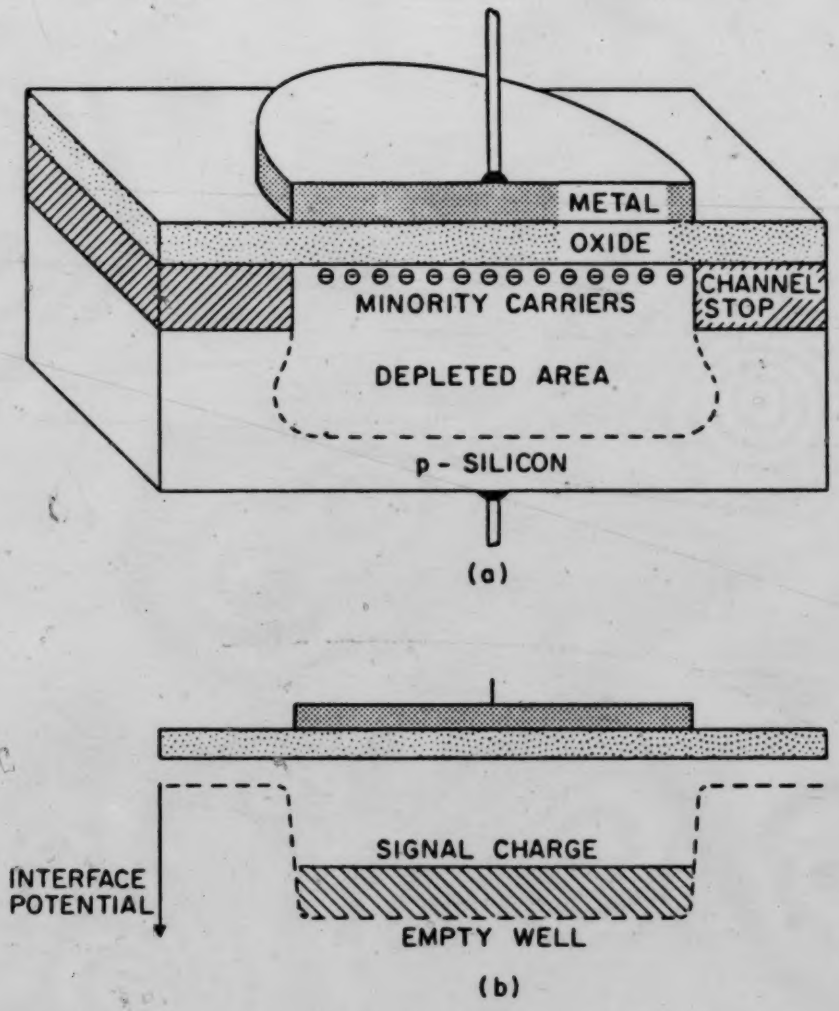

Figure 15. a) MOS capacitor.
b) Potential well with signal change.

the MOS capacitor, a region depleted of free carriers is formed due to the repulsion of the majority carriers (holes in p-type doped semiconductors) away from the interface. A potential well is thus formed at the oxide-semiconductor interface which accumulates and stores any minority carriers (electrons) which are generated at the interface either thermally or by incident photons. Lateral diffusion of the walls of the potential well is prevented by a channel stop made of semiconductor material of the same polarity as the semiconductor (p-type doped), but doped a few orders of magnitude greater. This almost conducting material keeps the potential of the surrounding oxide-semiconductor interface close to zero.

If two MOS capacitors are placed in very close proximity such that their depletion regions overlapped and their potential wells partially merged, any previous accumulation of mobile minority charge will ultimately reside at the MOS capacitor whose positive interface potential is the greatest (Figure 16 t_1). Therefore, the mobile minority charge, or charge packet, could be transferred to a neighboring MOS capacitor by applying a greater positive potential to the neighboring capacitor's electrode (Figure 16 t_2 to t_3). Then, by decreasing the positive potential on the electrode of the capacitor where the charge packet initially resided, an essentially

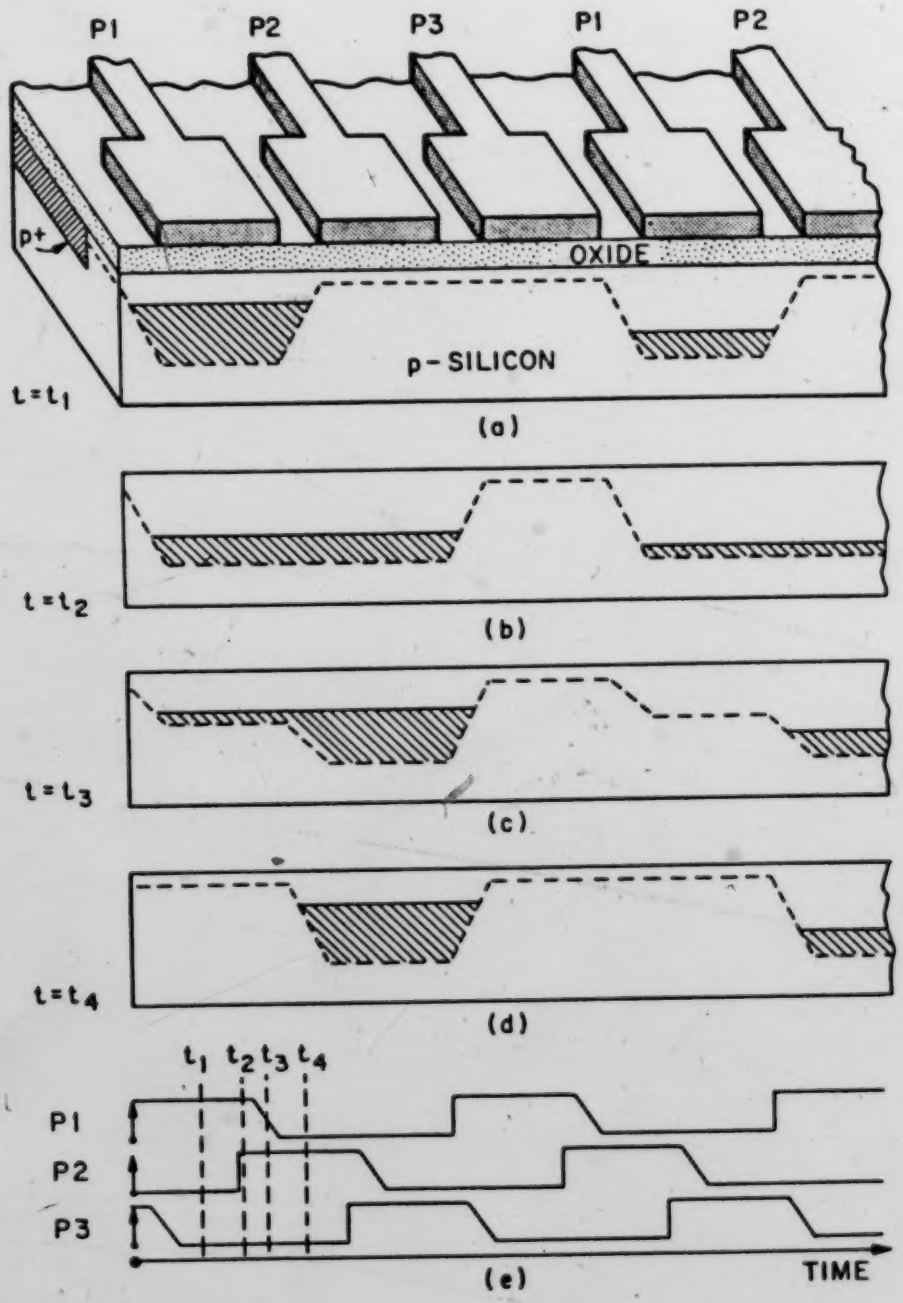

Figure 16. a) 3-phase n-channel CCD.
b,c,d) Potential wells depicting the transfer of charge.
e) Associated timing diagram.

complete transfer of the charge packet to the oxide-semiconductor interface of the neighboring MOS capacitor can be brought about (Figure 16 t_3 to t_4). Through the application of sequential clock pulses in phase with one another to the electrodes of a long series of MOS capacitors [71-73], discrete charge packets can be transferred down the series of MOS capacitors to an output detector.

The above qualitative picture applies to a surface-channel charge coupled device (SCCD) [74-76]. The term surface channel means that the charge packets are stored at the oxide-semiconductor interface where the well potential is a maximum. Due to interactions of the charge packets with fast interface states [77-82] and the rate at which charge can be transferred, it is preferable for optically generated signals to use a bulk or buried-channel charge coupled device (BCCD) [83-86]. BCCDs (Figure 17) contain an epitaxial [87] or ion-implanted layer [85] of semiconductor of opposite polarity to that of the substrate. This causes the maximum potential of the wells to be shifted away from the oxide-semiconductor interface and into the bulk of the semiconductor. When this layer is put in electrical contact with reversed biased input and output diodes, it will be drained of all mobile carriers. The depleted channel formed can then be

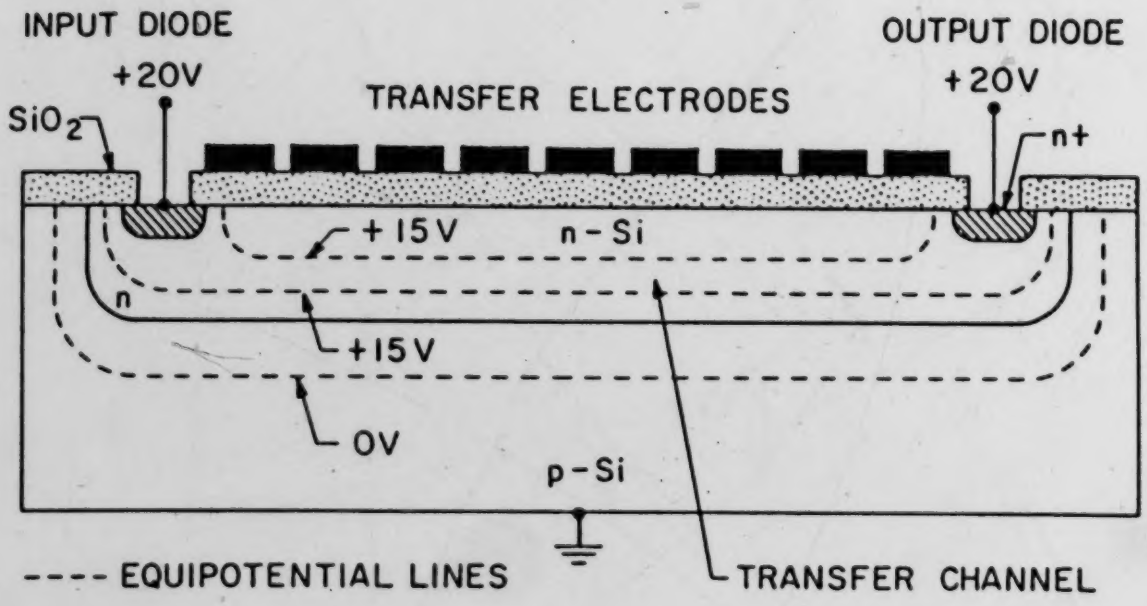

Figure 17. Buried channel CCD.

used to transport charge packets via moving potential wells created by modulating the potentials of the transfer electrodes with an appropriate pulse train.

The BCCD used in this research consisted of a bilinear arrangement in which every other MOS capacitor was connected via a transfer gate to the elements of one of two analog transport shift registers (Figure 18). When the transfer gate is opened all of the photoelements transfer their charge packets in parallel fashion to the two shift registers where they can be clocked out serially. This parallel transfer of charge allows for the simultaneous integration of all of the photons that have interacted with the photoelements.

Similar to a CCD is the device referred to as a photodiode array (PDA) [88] (Figure 19). A PDA consists of many photoelements with each photoelement being a diode and charged capacitor pair. Photons of light incident on the diodes create holes that migrate to the charged capacitor resulting in a gradual discharge of the capacitor; the discharge rate being proportional to the flux of incident light. To decode the charge/photon information, a multiplexer connects each individual photoelement (diode and capacitor pair), one at a time, to a voltage source. This voltage source recharges the capacitor to the original potential with the total current

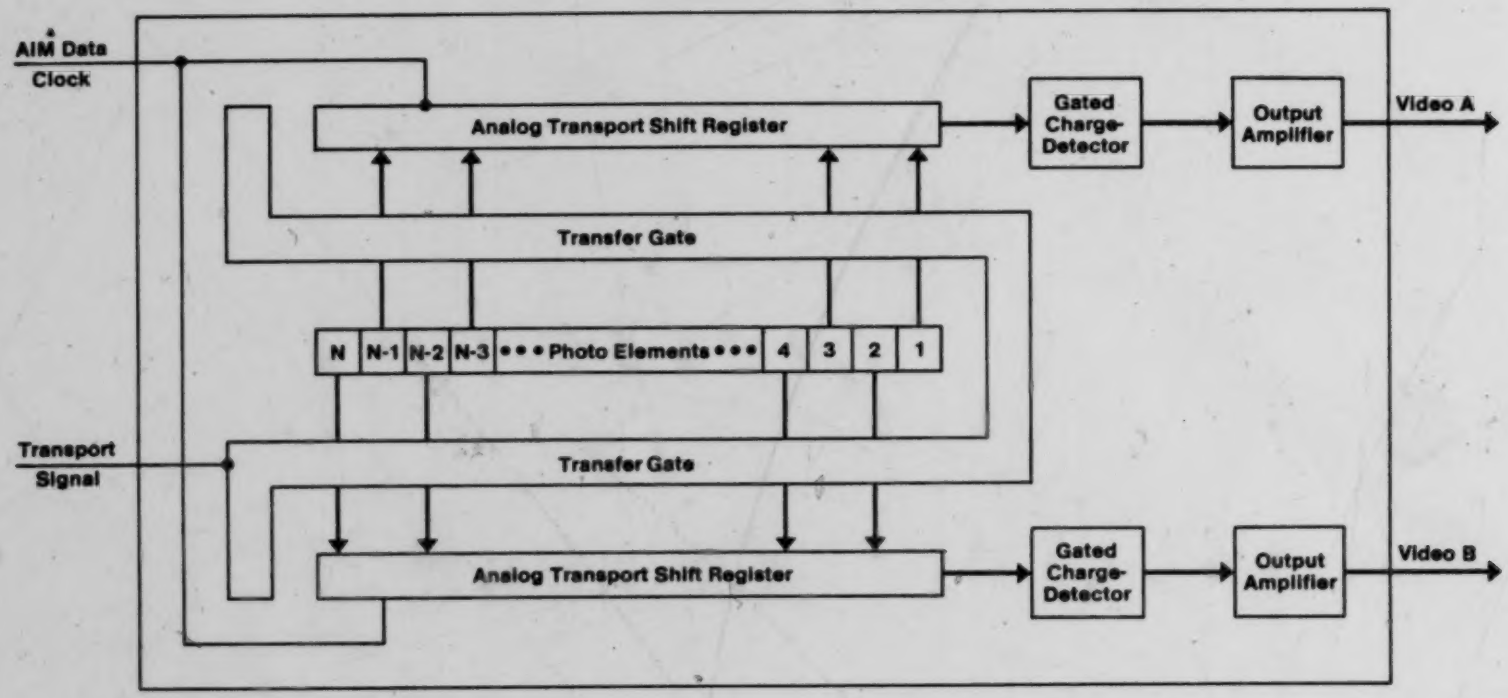

Figure 18. Bilinear arranged BCCD.

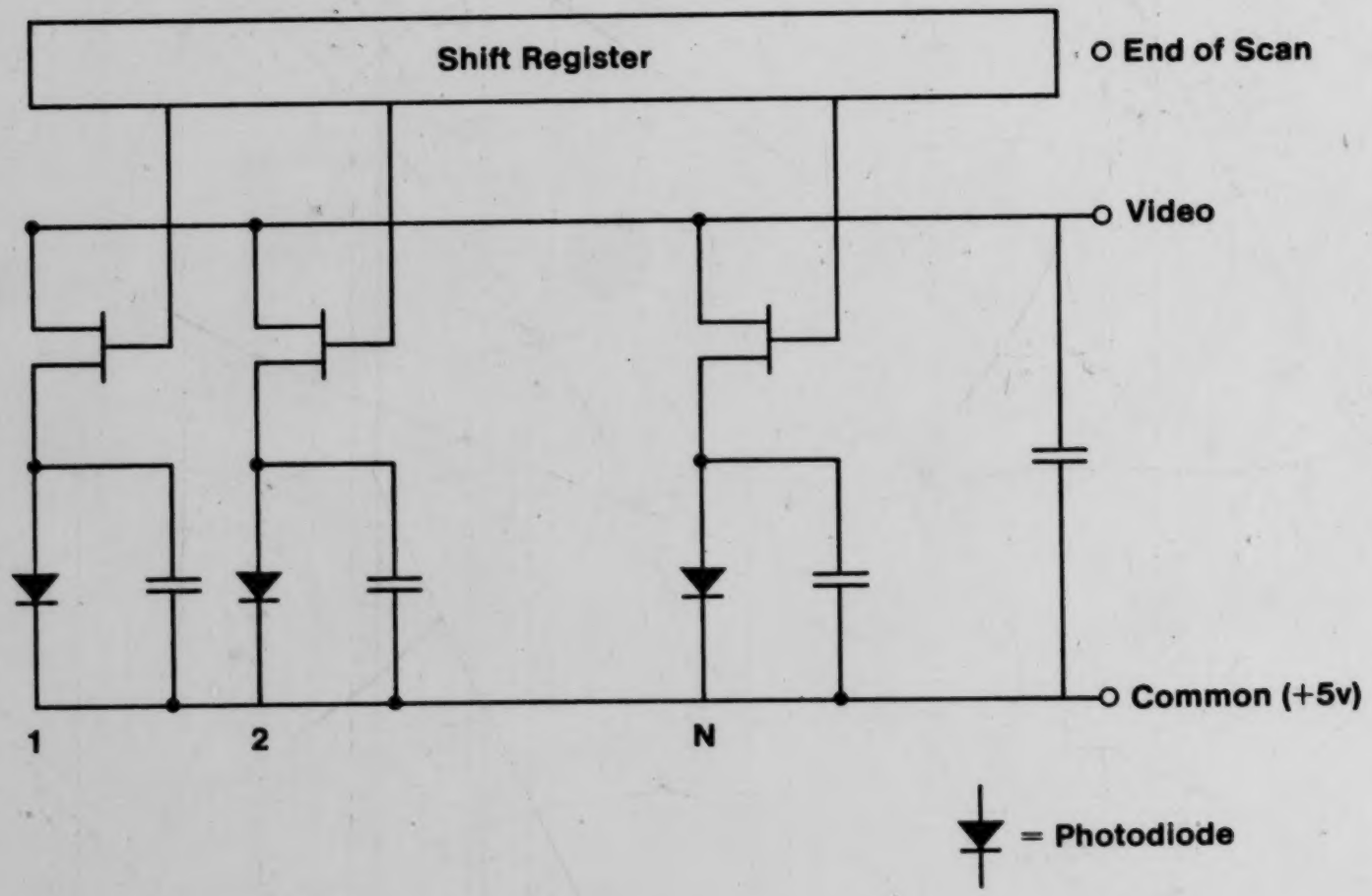

Figure 19. PDA schematic.

necessary to perform this function being measured. The multiplexer then connects the next photoelement to the voltage source and the process is repeated with each photoelement being read once in each multiplexed cycle. The CCD and PDA, while being similar in package, are thus very different in their corresponding modes of operation. The spectrum from a properly dispersed light source can be made to be incident on the photoelements of a PDA or a CCD. In the case of the CCD it is possible to obtain the spectrum of a discrete event such as that of a chemically generated cation species, due to the ability of the CCD to integrate all photoelements over the same time frame. There is then a transfer of this information, all at once, in parallel fashion to analog shift registers where it can then be serially clocked out and read. This is not possible with a PDA since each photoelement has to be read one at a time. In this case, a shutter between the light source and the PDA would be necessary to prevent the remaining photoelements from continuing to integrate incident light while the previous photoelements are being read. The most time consuming portion of the operation of a CCD or PDA is the conversion of the analog photoelement data to its digital equivalent and storage in a microprocessor. This would severely limit the shortest integration period of a PDA to a value well into the

millisecond range unless extraordinary circuitry is used. This lower limit is easily surpassed with the CCD whose integration period is solely dictated by the rate at which two pulses can be delivered, one to initiate and one to terminate the integration period. The present electronic lower limit to the integration period used in this research is approximately fifty-five microseconds which is set by a twenty megahertz clock. The ultimate lower limit of integration is determined by the intensity of the light source [84,89-93].

While it is not intended here to discredit the PDA, it is apparent that the CCD will possibly replace the PDA due to its ability to integrate discrete and very short events and the simplicity with which it can be interfaced with modern, inexpensive microprocessors. This is true for virtually all presently existing commercial applications.

CHAPTER 4

RESULTS AND DISCUSSION

The usual detector utilized to perform MSRS in the u.v.-visible spectral region is the photomultiplier tube as discussed previously. It has been the purpose of this research to replace this type of detector and its associated circuitry with the new CCD detector. In order to assess the performance of this new spectrophotometer, it is first necessary to discuss the electronic circuitry and associated elements of the former case. It will be subsequently demonstrated that the selection of a CCD as a detector is advantageous not only from the point of view of multi-wavelength monitoring, but also due to simplifications in the electronics, experimental procedure, and a gain in versatility.

The experimental components utilized in MSRS are shown in Figure 20. In a complete kinetic analysis of an electron transfer system, it must be realized that there are probably several intermediate species generated homogeneously after the initial electron transfer. It is thus necessary to obtain a spectrum over the entire spectral range available to see if any of these species

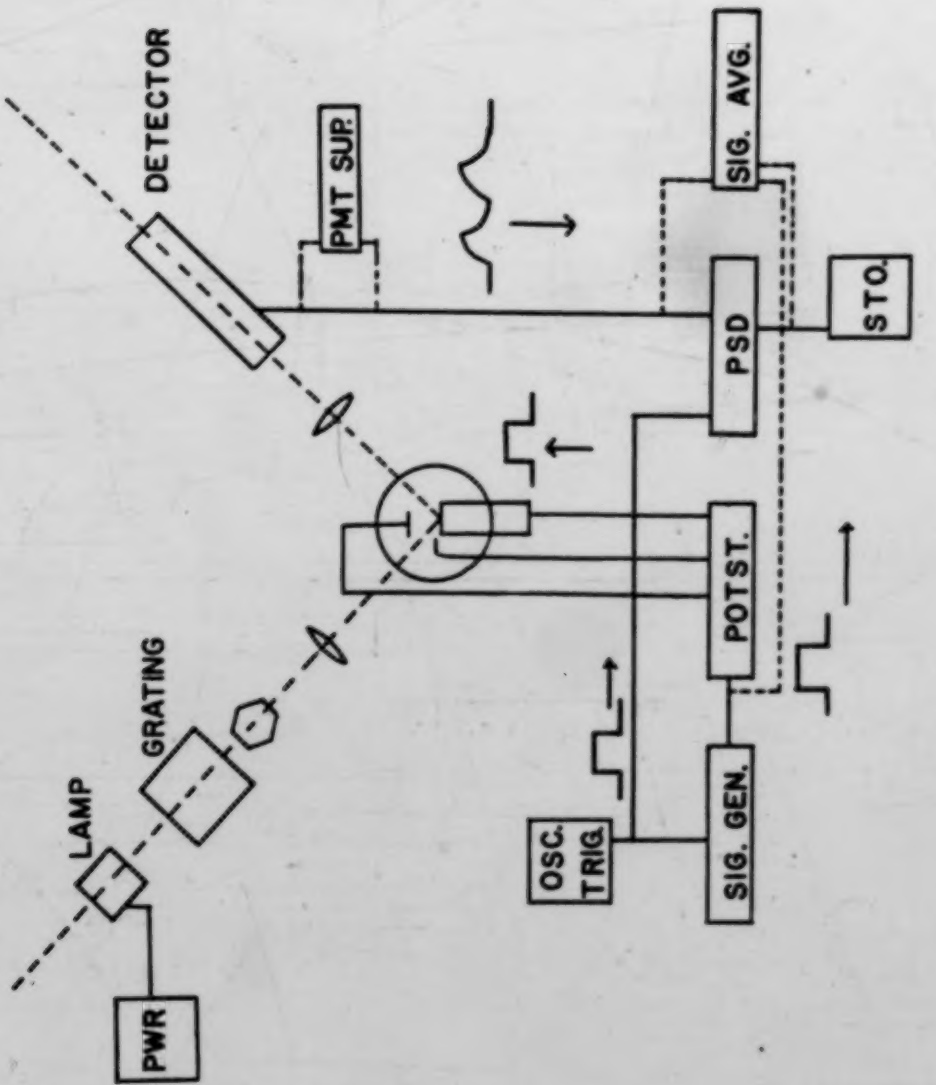

Figure 20. Experimental apparatus used to perform reflectance experiments with a PMT.

are chromophores. The kinetics of each chromophore may then be investigated with absorbance-time transients obtained at the appropriate wavelengths. The spectrum is first obtained by modulating the electrode with a square wave (typically 40 Hz) around the half-wave potential of the redox reaction. This is usually performed from a base potential where there is no electron transfer reaction to one where the reaction is diffusion controlled. If the new conjugate redox species absorbs the incident radiation, then there will appear a 40 Hz modulation in the reflected beam. The beam is incident on the PMT so that its output may be deconvoluted using phase sensitive detection to extract the small signal associated with the modulation. The phase sensitive detection system then provides a d.c. signal proportional to the r.m.s. amplitude of that modulation. This amplitude will be a maximum, obviously, at the λ_{max} of the chromophore.

In order to assure a relation between this d.c. output voltage and the desired $\Delta R/R$, it is necessary to use an electronic feedback circuit. The feedback circuit controls the voltage across the dynodes of the PMT. The circuit, which is given in Figure 21, allows the direct recording of $\Delta R/R$. It is designed to maintain a constant d.c. output regardless of the light intensity or wavelength response of the PMT. This means, effectively,

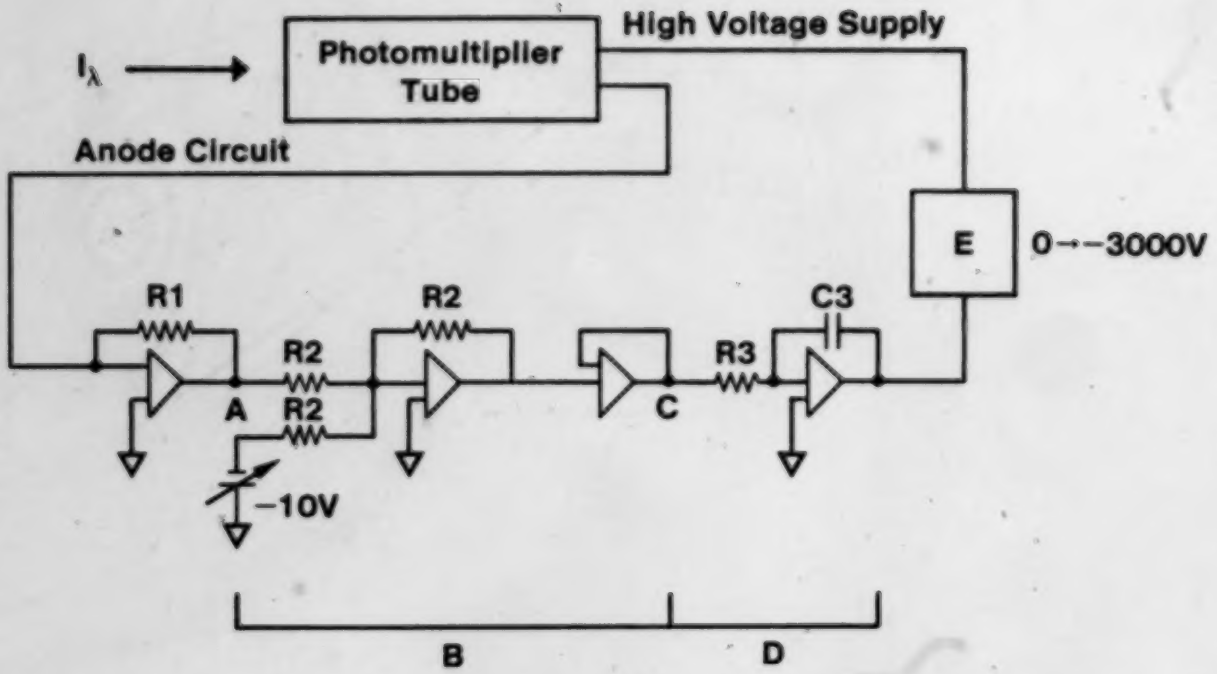

Figure 21. PMT feedback circuit.

that R is kept constant. Thus, if it is possible to detect ΔR with the same circuit by an a.c. sensitive amplifier, ΔR will be proportional to $\Delta R/R$ at all wavelengths, i.e. $\Delta R = \alpha \Delta R/R$ (n.b. if x=y for all x and y, x/c is proportional to y if c is a constant), where α is a constant of proportionality. The operation of the circuit, which is a dynamic feedback loop, is as follows: resistor R1 is chosen such that when a desired current flows in the anode output circuit of the PMT, +10 V will appear at the output, A, of the current follower. This +10 V is nulled by adding a constant -10 V with the summing amplifier and voltage follower of section B, thus making the total effective output equal to zero volts at point C. This voltage is integrated by the integrator of section D. This integrator has a time constant which is long compared to the electrode modulation frequency. Thus any perturbation in the light intensity due to the electrode modulation will pass unimpeded, while slowly changing signals will be effectively integrated. The output of the integrator is input to a programmable power supply, E, which drives the PMT. Any positive voltage appearing at the input to the programmable power supply will cause the supply voltage to the PMT to decrease. Conversely, any negative input voltage will cause an increase in the supply voltage to the PMT, thus completing

the mechanism for maintaining an effectively constant current through the PMT, and hence a constant d.c. voltage or R. The above explanation may be made quantitative by considering the following example. Assume that R1 has been adjusted so as to make the input to the integrator equal to zero volts while ß milliamps are flowing constantly in the PMT which is driven by a voltage γ V from the programmable power supply E. If the intensity of the light incident on the PMT were now to begin to increase, possibly due to the appearance of a strong spectral line in the slit while the wavelength is being scanned, the current in the PMT would increase by some value, di. The current follower would respond by increasing its +10 V output by Xdv V to 10 + Xdv V (X is the gain of the current follower). The net voltage at output C of the voltage follower is thus -10 + 10 - Xdv V or -Xdv V. This voltage is integrated and a positive voltage, $\frac{1}{(R3)(C3)} \int_0^t Xdv = X'$ V appears at the input to the programmable power supply. This positive input causes the programmable power supply to decrease the supply voltage by γ - X' V to the PMT until the extra current, di, decreases sufficiently such that the input to the programmable power supply returns to zero. Thus, the circuit maintains a constant d.c. output at all light levels and/or wavelengths for any slowly varying PMT

response. In order to simultaneously obtain ΔR, the feedback circuit is tapped at point C and the signal is processed utilizing phase sensitive detection instrumentation. The phase sensitive detection instrumentation is driven at a given frequency of detection by a reference signal, which is the same as that being used to modulate the potential of the optical working electrode. With proper adjustment of any phase difference between the electrogenerated signal and the reference signal, the phase sensitive detection instrumentation is able to amplify almost exclusively that portion of the electrogenerated signal occurring at the reference frequency. The phase sensitive detection instrumentation then provides a d.c. output voltage level which is proportional to the r.m.s. amplitude of the electrogenerated signal. If the wavelength is scanned as the optical working electrode potential is modulated, the resultant spectrum of the electrogenerated species is recorded.

From the foregoing discussion, it is apparent that the electronic circuitry and instrumentation utilized to obtain the spectrum of an electrogenerated species with the PMT is more complex than with a CCD. In order to maximize the signal to noise ratio, there is also quite a bit of "fine tuning" necessary in the case of the PMT.

This "fine tuning" can become quite arduous at times as opposed to a simple adjustment of the slit width when using the CCD. Not only does it require a relatively long time to record a spectrum with the PMT, but it should be noted that the spectral information is not quantitative in terms of absolute quantities of chromophores present. Due to the squarewave modulation of the working electrode potential, the electrochemical system is not given enough time to relax back to its original conditions during the time the potential is returned to the base level. If asymmetrical square waves were used to overcome this problem, more serious problems with the phase sensitive detection circuitry would be injected. This lack of recovery at the electrode surface causes the electrochemical system to quickly achieve a steady state condition, thus stripping the spectrum of any information with respect to the relative amounts of the several species which may be present with different kinetic characteristic times.

The cyclic voltammogram of 2,6-di-tert-butyl-4(4-methoxyphenyl)-aniline is given in Figure 22. The electrogenerated spectrum of the cation radical obtained with the CCD and with the PMT-phase sensitive detection instrumentation is given in Figures 23 and 24, respectively. By comparing these two spectra, it is quite obvious that the square wave modulation of the

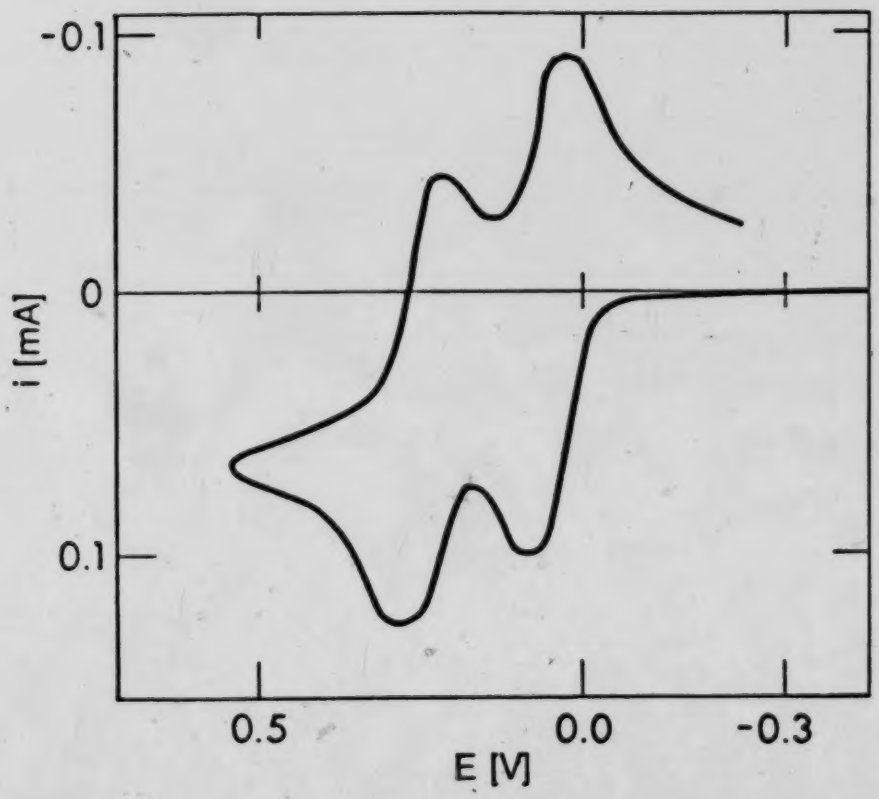

Figure 22. Cyclic voltammogram of 2,6-di-tert-butyl-4,(4-methoxyphenyl)-aniline in acetonitrile/0.1 M tetra-n-butylammonium tetrafluoroborate, scan rate 100 mV/s, conc. 1.0 mM.

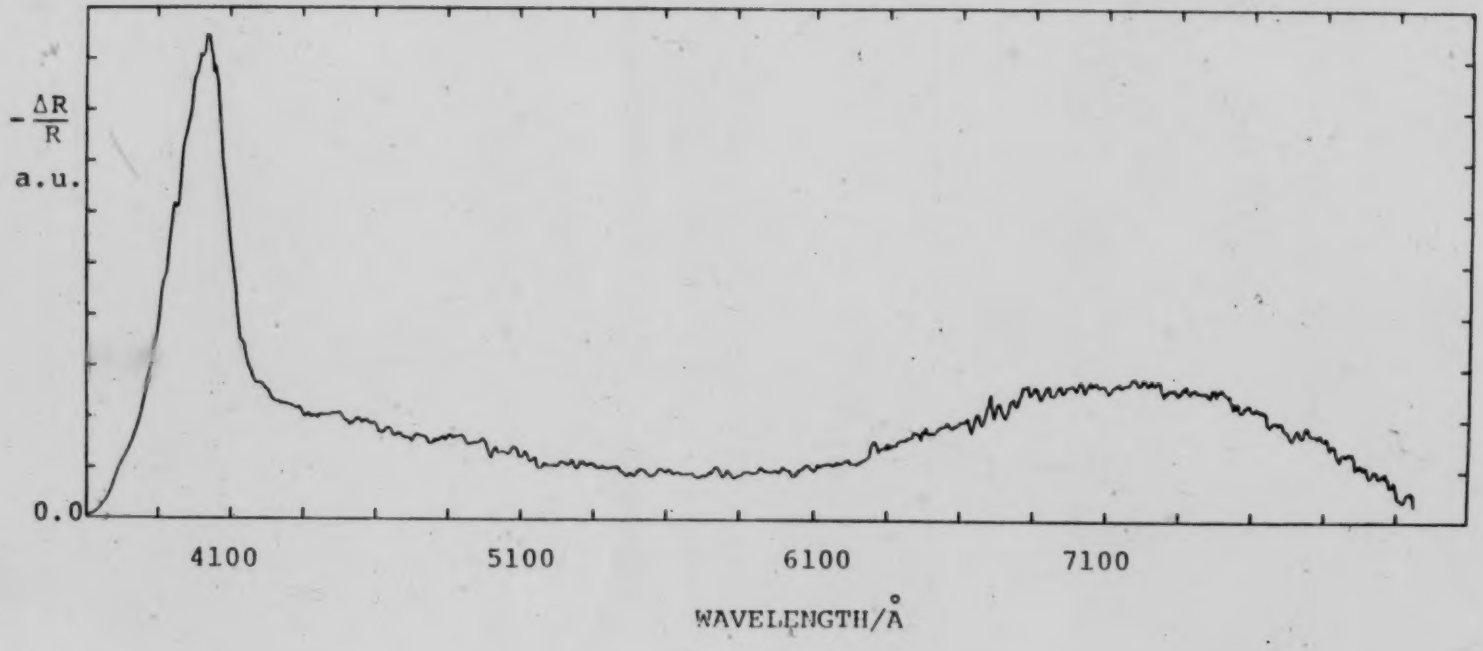

Figure 23. Spectrum of the 2,6-di-tert-butyl-4-(4-methoxyphenyl)-aniline cation radical obtained with a CCD, potential step from -300 mV to +200 mV vs Ag/Ag^+, 0.1 M tetra-n-butylammonium tetrafluoroborate in acetonitrile.

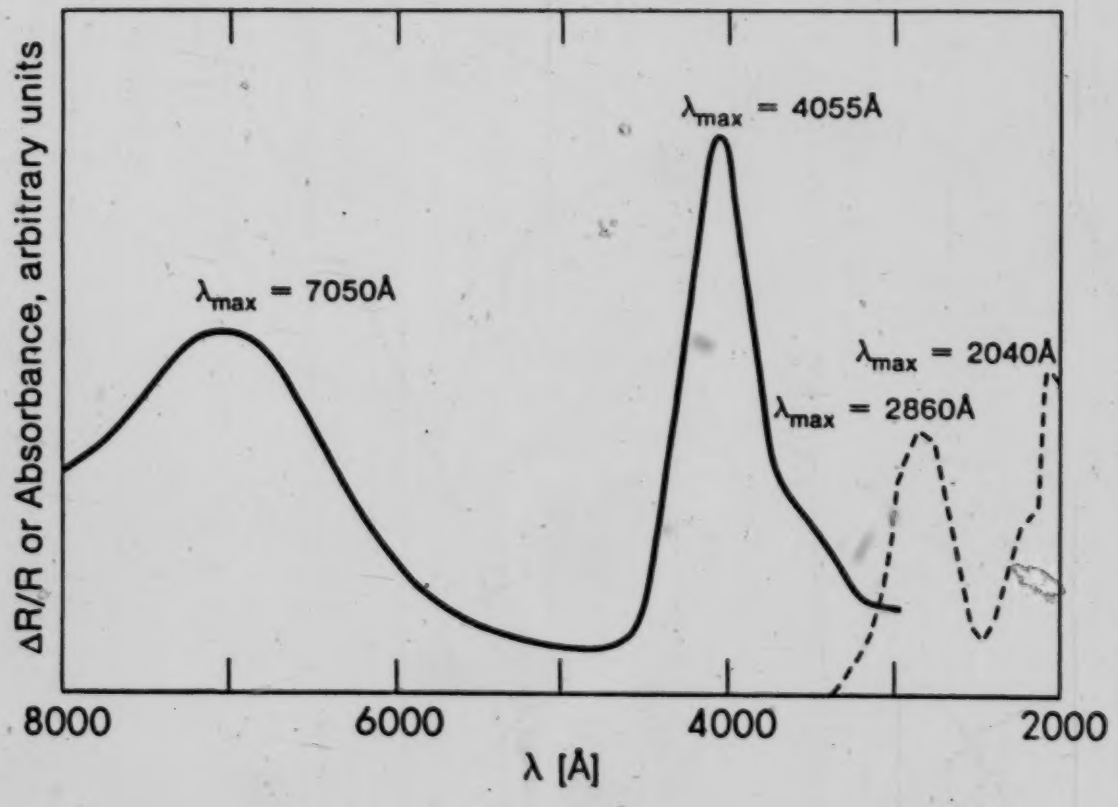

Figure 24. Spectrum of the 2,6-di-tert-butyl-4-(4-methoxyphenyl)-aniline cation radical obtained with a PMT (conditions same as Figure 23).

working electrode potential in the latter technique can highly distort the spectrum of the electrogenerated species. The relative heights of the two absorption maxima are quite different in the two cases. If the PMT is replaced with the CCD, it is no longer necessary to use the relatively complex phase sensitive detection instrumentation to acquire the spectrum of the electrogenerated species, and hence square wave modulation of the working electrode potential is avoided. Due to the ability of the CCD to integrate any incident light simultaneously on all photoelements, it is only necessary to use signal averaging (to simply increase the signal-to-noise ratio) to acquire the spectrum of an electrogenerated species.

To perform the experiment using a CCD as a detector, the light from a source which has been reflected off the optical working electrode is properly dispersed (via a grating) with the resulting spectrum being made incident on the photoelements of the CCD. The CCD is allowed to "free run", in effect, discarding all incident light information and clearing itself, until it is time to record a spectrum. At this time the potential of the working electrode is pulsed to the desired potential and the spectrum of the electrogenerated species is recorded and stored. Following the data acquisition, the potential

of the working electrode is returned to its base rest potential and held there for a suitable amount of time. For the electrochemically reversible compounds studied in this research, it was only necessary to return to the base potential for 4 seconds in order to achieve the original conditions. This time represents a duty cycle of 1.6%, enough to reach to within 0.03% of the initial conditions. Due to the small magnitude of $\Delta R/R$, it was necessary to signal average approximately 256 separate spectra to obtain a good quality spectrum of the electrogenerated species. In contrast to the method utilizing the PMT and phase sensitive detection instrumentation, the resultant spectrum in this case is quantitative.

In order to complete the kinetically quantitative MSRS experiment after having obtained the spectrum of the electrogenerated species using phase sensitive detection and the PMT, it would now be necessary to select a few wavelengths at which $\Delta R/R$ - t transients would be recorded. The transient work would be carried out using signal averaging similar to that presented above using the CCD, but the resultant information, resembling the kinetic transient of Figure 25, would only be obtained at one wavelength. Conversely, in order to reconstruct an entire spectrum having quantitative information, it would be

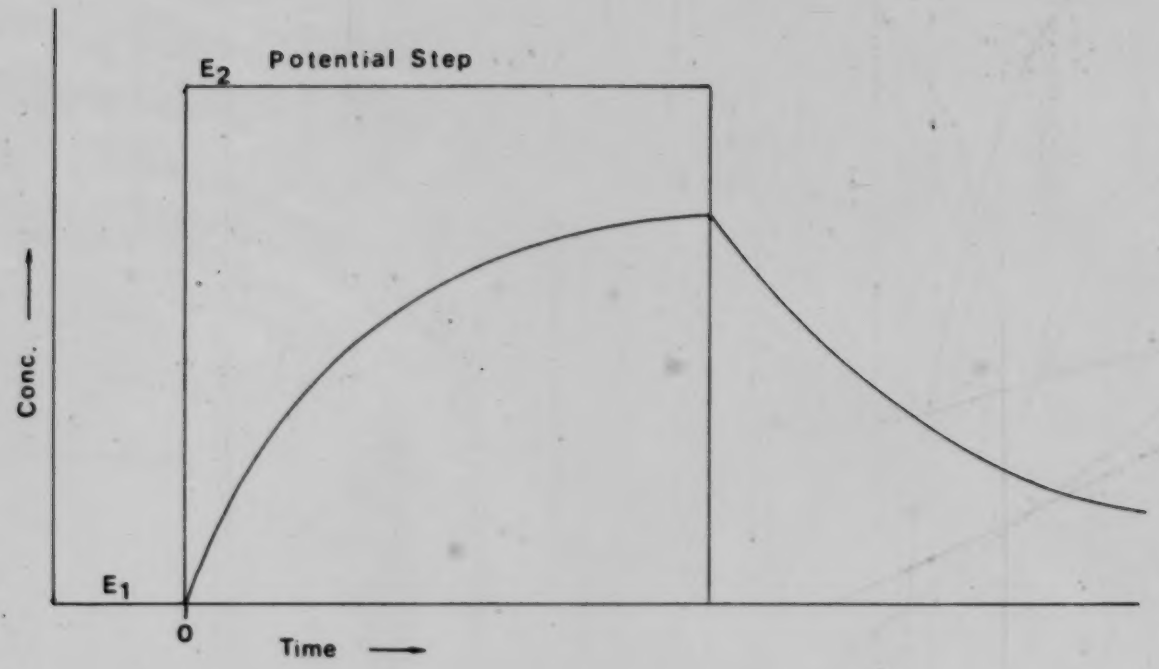

Figure 25. Concentration profile of electrogenerated species vs. time.

necessary to signal average at many wavelengths which at best is very time consuming. The few transients recorded at specific wavelengths present the absorbance profiles of the electrogenerated species as a function of time. This can easily be accomplished with the CCD by using a small light integration period and taking only a few spectra. These spectra, all of the same small integration period, are taken at different time intervals after the initiation of the potential step. In the present application, there are three spectra taken per potential pulse, each separated by 20 ms with 20 ms being the minimum amount of time needed to shift out and store one spectrum. Not only is the acquired data sufficient for quantitative work, but it is recorded as a spectrum, thus expanding the usual two dimensional information from that of time versus absorbance to three dimensions by including wavelength. Data is given in Table 1 for the electrogenerated radical cation of 1,4-dimethoxy-9,10-diphenylanthracene. The reflectance experiments were carried out using both the PMT and the CCD as detectors. The data obtained with the CCD corresponds only to one wavelength, the same wavelength at which the data using the PMT was obtained (6530 Å). Using the data in Table 1 and equation 54 from the theoretical section, the diffusion coefficients calculated for the radical cation using the PMT and CCD

Table 1. MSRS data obtained with a PMT and CCD of the 1,4-dimethoxy-9,10-diphenylanthracene cation radical at 6530 Å (conditions same as Figure 27).

PMT		CCD	
$\Delta R/R / 10^{-2}$	Time (ms)	$\Delta R/R / 10^{-2}$	Time (ms)
1.01	20	3.52	62.5
1.44	40	3.11	47.5
1.71	60	2.65	32.5
1.98	80	1.95	17.4
2.17	100	0.71	1.25
Conc. = 1mM		Conc. = 2mM	

are in very good agreement, differing by less than 0.1%. The cyclic voltammogram of 1,4-dimethoxy-9,10-diphenylanthracene along with the five spectra taken using the CCD are presented in Figures 26 through 31. The spectra were taken with a light integration period of 5 ms using a 35 W quartz-halogen lamp.

The graph in Figure 32 is a plot of $\Delta R/R$ versus the duration of the integration period. Each value of $\Delta R/R$, derived from a different spectrum, was taken 47.5 ms after the initiation of the potential step. It is clear from this graph that the 5 ms integration period used is close to the minimum achievable with the 35 W quartz-halogen source and the dispersing optics used herein. If this source were replaced with a 200 W mercury-xenon lamp, for instance, the integration period should be able to be decreased considerably. It is surmised that since $\Delta R/R$ only decreased by a factor of 7 over a two orders of magnitude decrease in integration period, the common 200 W mercury-xenon lamp should provide enough flux to allow an integration period of 50 μs to be achieved. Work in this area is continuing.

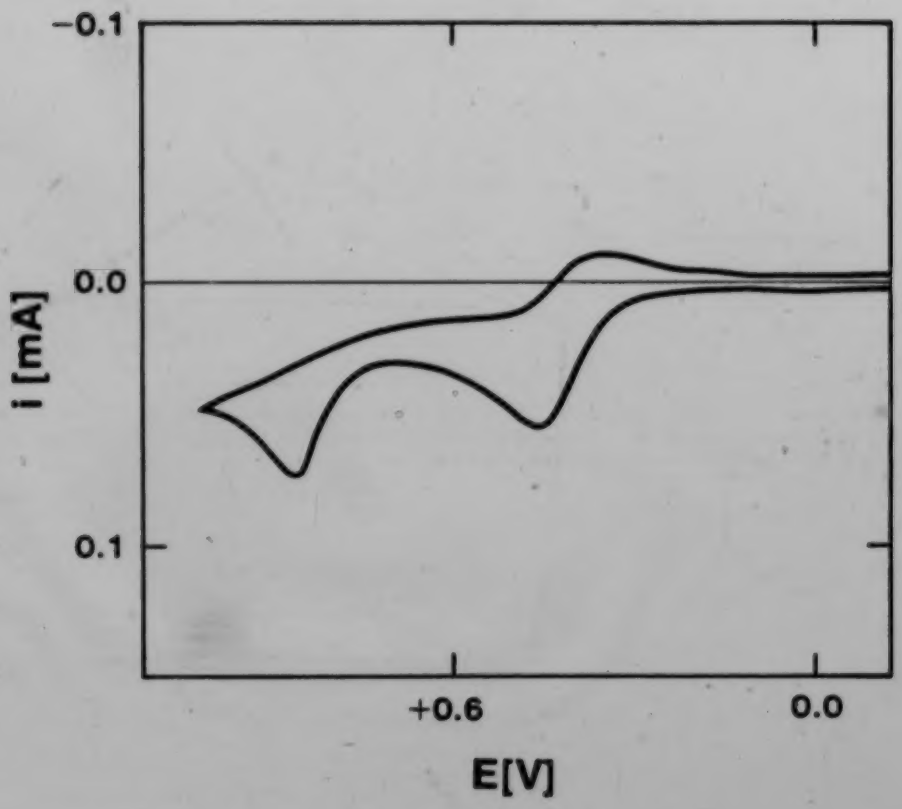

Figure 26. Cyclic voltammogram of 1,4-dimethoxy-9,10-diphenylanthracene in acetonitrile/0.1 M lithium perchlorate, scan rate 100 mV/s, conc. 1.0 mM.

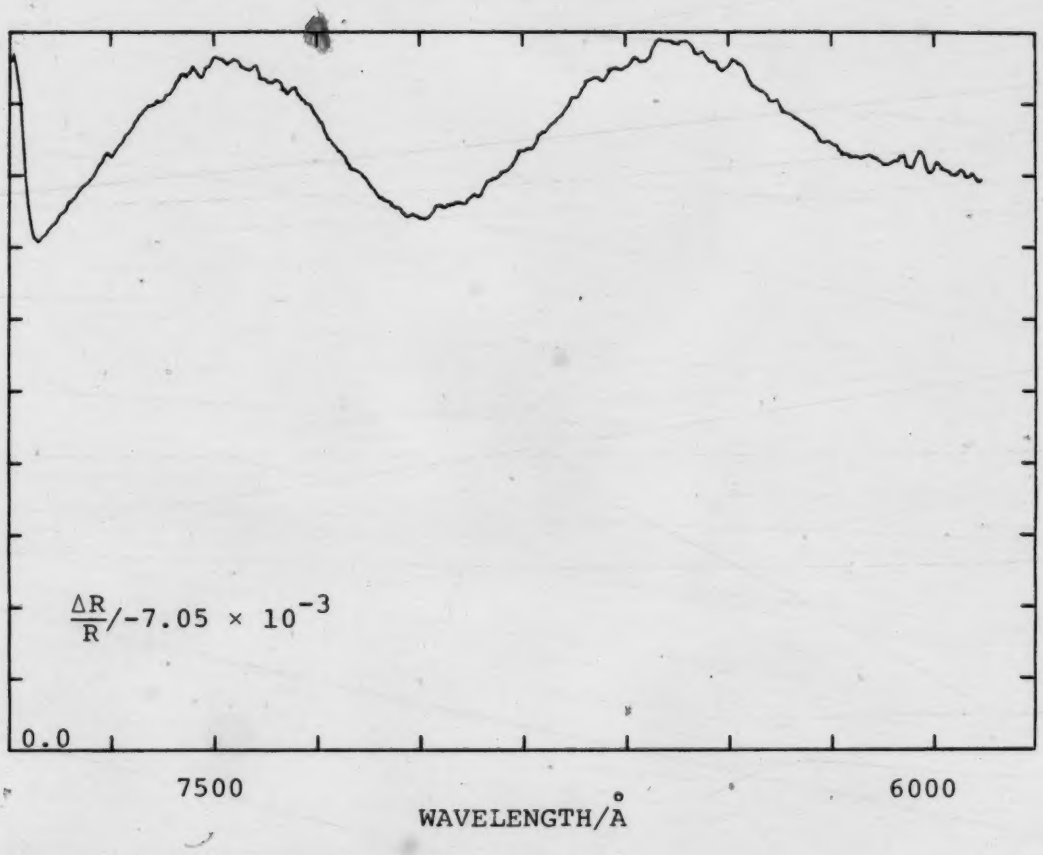

Figure 27. Spectrum of 1,4-dimethoxy-9,10-diphenyl-anthracene cation radical in acetonitrile/0.1 M lithium perchlorate, potential step from 0.0 mV to 600 mV vs Ag/Ag^+, conc. 1.0 mM, integration period - 5 ms, integration initiated at 60 ms.

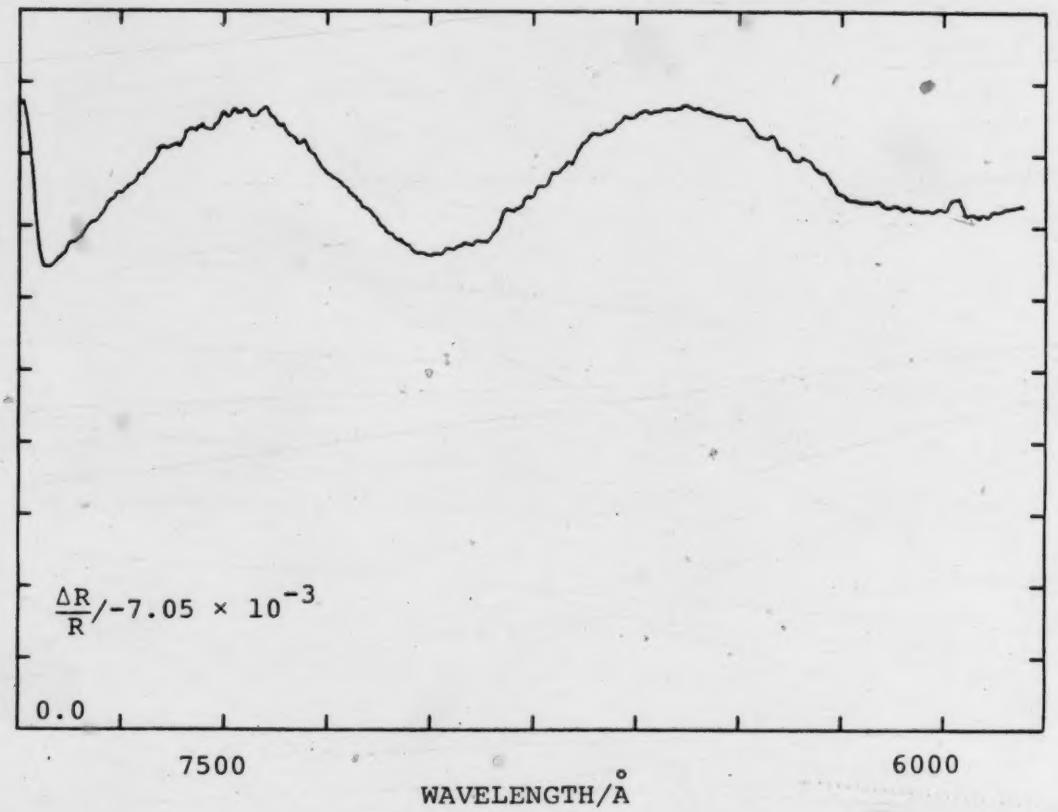

Figure 28. Conditions same as Figure 27 except integration initiated at 45 ms.

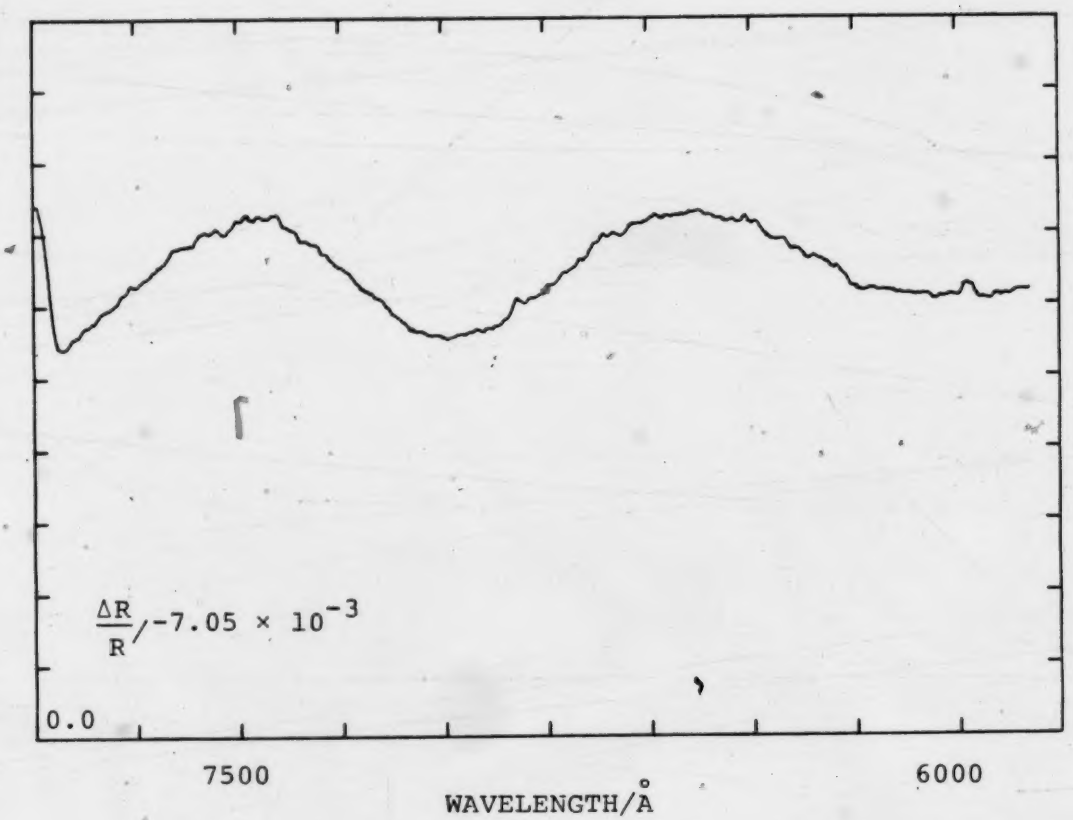

Figure 29. Conditions same as Figure 27 except integration initiated at 30 ms.

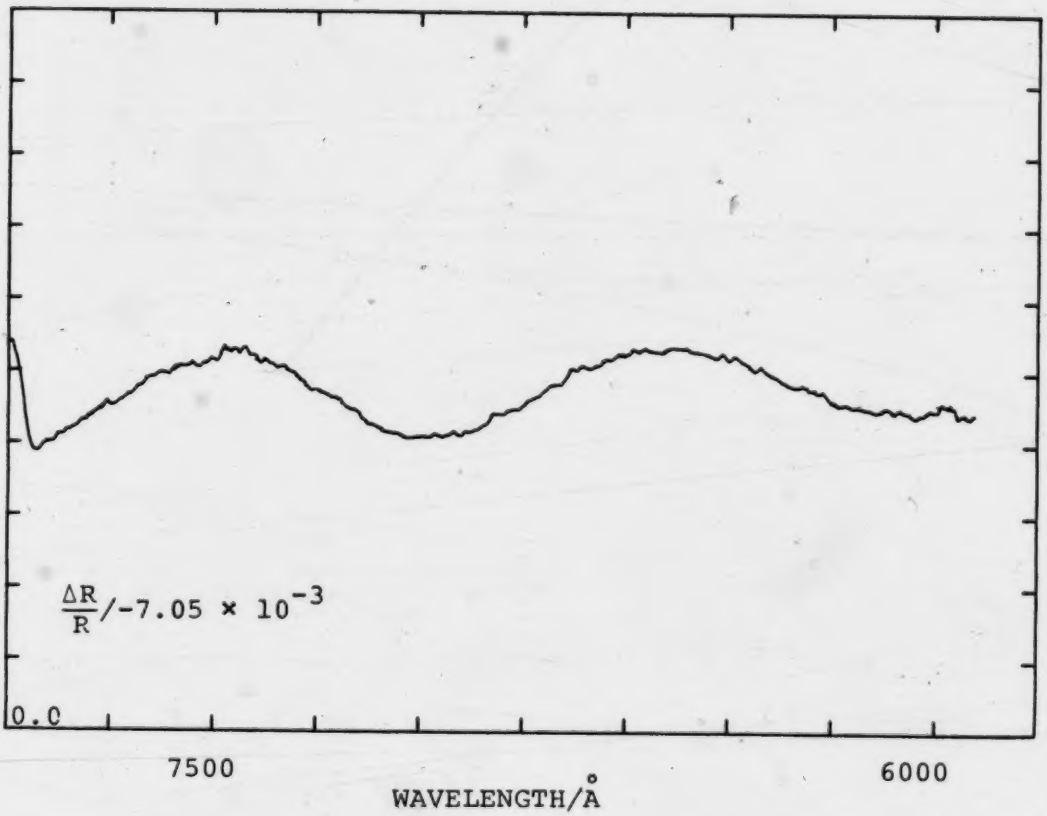

Figure 30. Conditions same as Figure 27 except integration initiated at 15 ms.

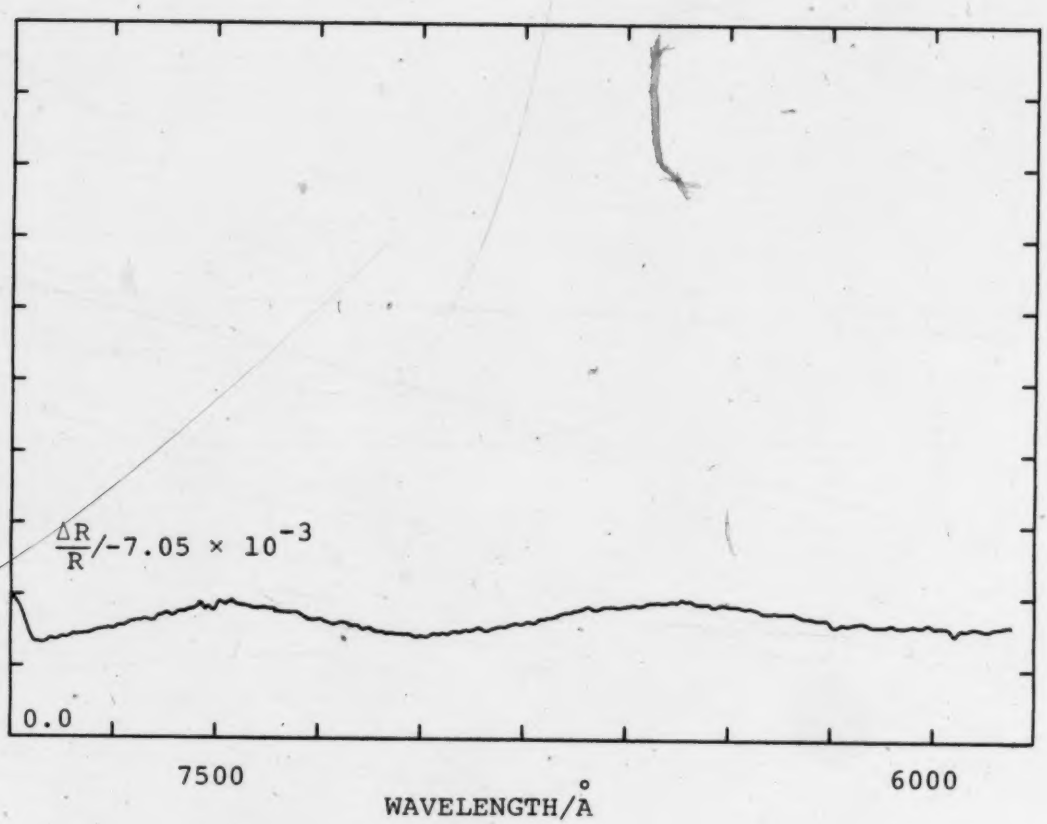

Figure 31. Conditions same as Figure 27 except integration initiated at 0.0 ms.

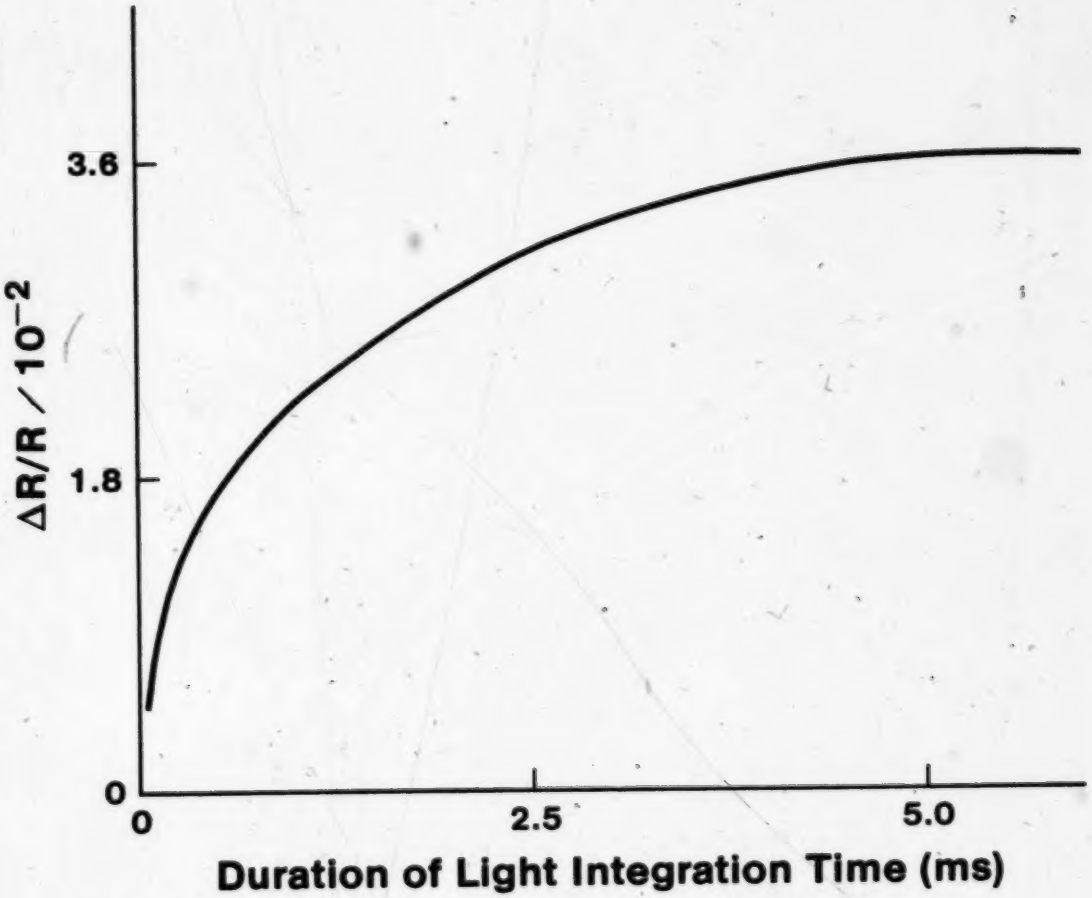
3.6
1.8
0
$\Delta R/R / 10^{-2}$
0
2.5
5.0
Duration of Light Integration Time (ms)

Figure 32.

4.1 Conclusion

In MSRS experiments in the u.v.-visible region, the replacement of the PMT with a CCD is a viable and desirable alternative. Not only does the CCD allow for the acquisition of a quantitative spectrum of the electrogenerated species of interest, but the instrumentation used to acquire this spectrum is less complex and the overall acquisition is less time consuming and provides more information. In the case of reactions preceeding or following the production of the electrochemical species in which there are other light absorbing species, the rapid and simultaneous multi-wavelength monitoring of such reactions can provide highly precise and complete homogeneous kinetic information. It should also be noted that the use of the microprocessor data acquisition system described herein to perform the reflectance experiment is not limited to this purpose and may be used in other electrochemical experiments in which the rapid acquisition of data is desirable.

A future and slightly more complex application of the CCD in reflectance electrochemical experiments is presently being realized in our laboratory. Through the utilization of direct memory access circuitry, it will be possible to shift out and store the 50 μs light integration period spectra in approximately 30 μs, thus

allowing for the acquisition of many individual spectra per potential step. This will enable the production of three dimensional electrochemical information (absorbance versus time versus wavelength) to be completed after signal averaging only one set of scans (the number of scans, of course, being determined by the molar absorptivity of the absorbing species). This is desirable in the analysis of irreversible systems in which the reactants tend to deplete quite rapidly, especially in biochemical systems where the total amount of substrate may be limited.

BIBLIOGRAPHY

1. T. Kuwana, Ber. Bunsenges. Phys. Chem. 77, 858 (1973).
2. W.R. Heineman, Anal. Chem. 50, 390A (1978).
3. H.B. Mark and B.S. Pons, Anal. Chem. 38, 119 (1966).
4. W.N. Hansen, R.A. Osteryoung and T. Kuwana, J. Am. Chem. Soc. 88, 1062 (1966).
5. W.N. Hansen, R.A. Osteryoung and T. Kuwana, Anal. Chem. 38, 1180 (1966).
6. B.S. Pons, J. Manson, L. Winstron and H.B. Mark, Anal. Chem. 39, 685 (1967).
7. A. Prostak, H.B. Mark and W.N. Hansen, J. Phys. Chem. 72, 2576 (1968).
8. N. Winograd and T. Kuwana, J. Electroanal. Chem. 23, 333 (1969).
9. D.E. Tallant and D.H. Evans, Anal. Chem. 41, 835 (1969).
10. R. Memming and F. Mollers, Symp. of the Faraday Soc. 4, 145 (1970).
11. H.B. Mark and E. Randall, Symp. of the Faraday Soc. 4, 157 (1970).
12. N. Winograd and T. Kuwana, Anal. Chem. 43, 252 (1971).

13. D. Laser and M.A. Ariel, J. Electroanal. Chem. 41, 381 (1973).

14. T. Kuwana and N. Winograd in A.J. Bard (Ed.), "Electroanalytical Chemistry", Vol. 7, Marcel Dekker, New York, 1974, p. 1.

15. J.F. Goely, A.M. Yacynych, H.B. Mark and W.R. Heineman, J. Electroanal. Chem. 103, 277 (1979).

16. T. Kuwana, R.K. Darlington and D.W. Leedy, Anal. Chem. 36, 2023 (1964).

17. J.W. Strojek and T. Kuwana, J. Electroanal. Chem. 16, 471 (1968).

18. J.W. Strojek, T. Kuwana and S.W. Feldberg, J. Am. Chem. Soc. 90, 1353 (1968).

19. T. Osa and T. Kuwana, J. Electroanal. Chem. 22, 389 (1969).

20. N. Winograd, H. Blount and T. Kuwana, J. Phys. Chem. 73, 3456 (1969).

21. G.C. Grant and T. Kuwana, J. Electroanal. Chem. 24, 11 (1970).

22. H.N. Blount, N. Winograd and T. Kuwana, J. Phys. Chem. 74, 3231 (1970).

23. W. Heineman and T. Kuwana, Anal. Chem. 43, 1075 (1971).

24. W. Heineman and T. Kuwana, Anal. Chem. 44, 44 (1972).

25. T. Kuwana and W.R. Heineman, Acc. Chem. Res. 9, 241 (1976).

26. W. Plieth, Symp. of the Faraday Soc. 4, 138 (1970).

27. A.W.B. Aylmer-Kelly, A. Bewick, P.R. Cantrill and A.M. Tuxford, Discuss. Faraday Soc. 56, 96 (1973).

28. A. Bewick, J.M. Mellor and B.S. Pons, Electrochim. Acta 23, 77 (1978).

29. R.L. McCreery, R. Pruiksma and R. Fagan, Anal. Chem. 51, 749 (1979).

30. J.F. Tyson and T.S. West, Talanta 26, 117 (1979).

31. R. Pruisksma, J. Electroanal. Chem. 144, 147 (1980).

32. C.E. Baumgartner, G.T. Marks, D.A. Alkens and H.H. Richtal, Anal. Chem. 52, 267 (1980).

33. A. Bewick, J.M. Mellor and B.S. Pons, Electrochim. Acta 25, 931 (1980).

34. J.P. Skully and R.L. McCreery, Anal. Chem. 52, 1885 (1980).

35. J.S. Mayausky and R.L. McCreery, Anal. Chem. 55, 308 (1983).

36. A.S. Hinman, J.F. McAleer and B.S. Pons, J. Electroanal. Chem., in press (1983).

37. D. Laser and M. Ariel, J. Electroanal. Chem. 35, 405 (1972).

38. A. Trifonov and I. Schopov, J. Electroanal. Chem. 35, 415 (1972).

39. T. Takamura, K. Takamura and E. Yeager, J. Electroanal. Chem. 29, 279 (1971).

40. M. Ito and T. Kuwana, J. Electroanal. Chem. 32, 415 (1971).

41. F.M. Hawkridge and T. Kuwna, Anal. Chem. 45, 1021 (1973).

42. A. Bewick and A.M. Tuxford, Symp. of the Faraday Soc. 4, 114 (1970).

43. A. Bewick and A.M. Tuxford, J. Electroanal. Chem. 47, 255 (1973).

44. P.T. Kissinger and C.N. Reilley, Anal. Chem. 42, 12 (1970).

45. W.R.Heineman and T. Kuwana, Anal. Chem. 44, 1972 (1972).

46. A. Bewick and J.W. Russel, J. Electroanal. Chem. 132, 329 (1982).

47. A. Bewick, K. Kunimatsu, J. Robinson and J.W. Russel, J. Electroanal. Chem. 119, 175 (1981).

48. A. Bewick and K. Kunimatsu, Surf. Sci. 101, 131 (1980).

49. B. Benden, A. Bewick, C. Lamy and K. Kunimatsu, J. Electroanal. Chem. 121, 343 (1981).

50. T. Davidson, B.S. Pons, A. Bewick and P.P. Schmidt, J. Electroanal. Chem. 132, 329 (1982).

51. E.A. Blubaugh, A.M. Yacynych and W.R. Heineman, Anal. Chem. 51, 561 (1979).

52. G. Grant and T. Kuwana, J. Electroanal. Chem. 24, 24 (1970).

53. W. von Benken and T. Kuwana, Anal. Chem. 42, 1114 (1970).

54. A.J. Bard and L.R. Faulkner, "Electrochemical Methods", John Wiley and Sons, New York, 1980.

55. G. Doetsch in W.M. Fairbairn (Ed.), "Guide to the Applications of the Laplace and z-Transforms", Van Nostrand Reinhold Co., London, 1971.

56. G.B. Thomas and R.L. Finney in "Calculus and Analytic Geometry", Addison-Wesley Publishing Co., Massachusetts, 1979, p. 875.

57. C.K. Mann, J. O'Donnell and J. Ayers, Anal. Chem. 37, 1161 (1965).

58. H. Lund and P. Iverson in M. Baiymer (Ed.), "Organic Electrochemistry", Marcell Dekker, New York, 1973.

59. J.F. Coetzee and W.R. Sharpe, J. of Soln. Chem. 1, 77 (1972).

60. D. Lancaster in "TTL Cookbook", Howard W. Sams and Co., Inc., Indiana, 1981.

61. W.F. Kosonocky and D.J. Sauer, Electron. Des. 23, 58 (1975).

62. W.S. Boyle and G.E. Smith, Bell Syst. Tech. J. 49, 587 (1970).

63. G.F. Amelio, M.F. Tompsett and G.E. Smith, Bell Syst. Tech. J. 49, 593 (1970).

64. W.F. Kosonocky, in R. Melen (Ed.), "Charge-Coupled Devices: Technology and Applications", IEEE Inc., New York 1977.

65. M.F. Tompsett, G.F. Amelio and G.E. Smith, Appl. Phys. Lett. 17, 111 (1970).

66. M.J. Howes and D.V. Morgan (Ed.), "Charge-Coupled Devices and Systems", John Wiley and Sons, New York, 1979.

67. G.S. Hobson, "Charge-Transfer Devices", Edward Arnold Ltd., London, 1978.

68. J.D.E. Beynon and D.R. Lamb (Ed.), "Charge-Coupled Devices and Their Application", McGraw Hill Book Co. Ltd., London, 1980.

69. R. Lindner, Bell Syst. Tech. J. 41, 803 (1962).

70. S.M. Sze, "Physics of Semiconductor Devices", John Wiley and Sons, Inc., New York, 1969, p. 425.

71. W.E. Engeler, J.J. Tremann and R.D. Baertsch, Appl. Phys. Lett. 17, 469 (1970).

72. D.A. Sealer, C.H. Seguin and M.F. Tompsett, 1974 IEEE Intercon Tech. Papers, Session 2, p. 1.

73. R.L. Rodgers, 1974 IEEE Intercon Tech. Papers, Session 2, p. 3.

74. W.F. Kosonocky and J.E. Carnes, RCA Rev. 34, 164 (1973).

75. D.Y. Leopoldo, IEEE J. Solid-State Siccuits, SC-11, 214 (1975).

76. S.R. Shortes, W.W. Chan, W.C. Rhines, J.B. Barton and D.R. Collins, Appl. Phys. Lett. 24, 565 (1974).

77. A.M. Moshen, T.C. McGill, Y. Daimon and C.A. Mead, IEEE J. Solid-State Circuits, SC-8, 125 (1973).

78. J.E. Carnes and W.F. Kosonocky, Appl. Phys. Lett. 20, 261 (1972).

79. M.F. Tompsett, IEEE Trans. Electronic Devices ED-20, 45 (1973).

80. V.V. Pospelov, R.A. Suris, B.I. Fouks and R.Z. Hafizov, Tech. and Appl. of CCD 3, 31 (1976).

81. W.J. Bertram, A.M. Mohsen, F.J. Morris, D.A. Sealer, S.H. Seguin and M.F. Tompsett, IEEE Trans. Electronic Devices ED-21, 758 (1974).

82. A.M. Mohsen and M.F. Tompsett, IEEE Trans. Electronic Devices ED-21, 701 (1974).

83. J. McKenna and N.L. Schryer, Bell Syst. Tech. J. 52, 660 (1973).

84. J.E. Carnes and W.F. Kosoncky, RCA Rev. 33, 607 (1972).

85. R.H. Walden, R.H. Krambeck, R.J. Strain, J. McKenna, N.L. Schryer and G.E. Smith, Bell Syst. Tech. J. 51, 1635 (1972).

86. L.J.M. Esser, Electron. Lett. 8, 620 (1972).

87. L.J.M. Esser, CCD Appl. Conf. Proc. 269 (1973).

88. W.G. Nunn, R.E. Deny and W.R. Reynolds in "Multichannel Image Detectors", Y. Talmi (Ed.), American Chemical Society, Washington D.C., 1979, p. 135.

89. A.L. Solomon, 1974 IEEE Intercon Tech. Papers, Session 2, p. 2.

90. D.D. Wen, "Charge-Coupled Devices: Technology and Applications", R. Melen (Ed.), IEEE Inc., New York, 1977.

91. M.H. White, D.R. Lampe, F.C. Alaha and I.A. Mack, IEEE J. Solid-State Circuits SC-9, 1 (1974).

92. B.R. Holeman and P. Gardner, Tech. and Appl. of CCD 3, 98 (1976).

93. S.B. Campana, Tech. and Appl. of CCD 3, 119 (1976).

APPENDIX A

APPENDIX A

This is the software program used in the PERQ computer to analyze the data.

```
R{Program reads three files (test11,test22,test33) which are the R2, RØ, and dark current
respectively.  Program calculates ((R2-R3)-(RØ-R3))/(RØ-R3) which is equivalent to
delR/R.  Data is dumped to file t4 for bascomb plotting.  The real value of delR/R is
given by taking the plotted value in volts on the bascomb and treating as follows:The
maximum actual value of delR/R is printed on the screen after plotting on screen.
Program is also used to plot time resolved spectra (total of 6)}


program ccd1 (input,output,test1,test2,test3,test4,test5,test6,test7,test8,test9,test1Ø,
test11,test12,test13,test14,test15,test16)


label 1,2,3,4,5,6,7,8;

type
maxlen=1..2024;
card=text;
ar1-array[maxlen] of char;
ar2=array[maxlen] of integer;
ar3=array[maxlen] of real;

var
maann:integer;


imports screen from screen;

procedure delr;
```

```
label 1,2,3,4,5,6,7,8;

var ar,arr,arrrr,a2a,a2b,a2c,a3a,a3b,a3c,a4a,a4b,a4c,a5a,a5b,a6c,a6a,a6b,a6c:ar1;
     test1,test2,test3,test4,test5,test6,test7,test8,test9,test10,test11,test12,test13,te
     st14,test15,test16,test17,test18,trf,trfb,bb,cc,dd,ee,gg,hh,kkk,c,d,e,g,h,ydd,tddd,t
     dddd,t2,t3,t4,t5,t6,t22,t33,t44,t55,t66,t222,t333,t444,t555,t666:real;
     i,j,l,m,n,nn,oo,ooo:integer;
     k,kk,kkkk,k2,k3,k4,k5,k6,k2a,k2b,k2c,k3a,k3b,k3c,k4a,k4b,k4c,k5a,k5b,k5c,k6a,k6b,k6c
     :
     ar2;
     a,aa,aaaa,a2,a3,a4,a5,a6:ar3;

begin

writeln('Make sure spectra are in seq. test files in decreasing intensity');
writeln('Maximum values of data are +/- 500 for screen, and +/- 250 for
Bascomb hardcopy (-10.0 and 0.0 V).');
writeln('How many time resolved spectra are there? 6 maximum.');
readln(ooo);
writeln('Enter multiplier (real form).');
readln(kkk);
writeln('Enter no. of data points to cut off front end(integer). 2 is the
smallest number allowed.');
readln(nn);
writeln('Do you want to inspect the data before plotting?Type 1 for yes
or 0 for no');
readln(oo);

reset(test1,'test11');
reset(test2,'test22');
reset(test3,'test33');
reset(test4,'test44');
reset(test5,'test55');
reset(test6,'test66');
```

```
reset(test8,'test88');
reset(test9,'test99');
reset(test10,'test1010');
reset(test11,'test1111');
reset(test12,'test1212');
reset(test13,'test1313');
reset(test14,'test414');
reset(test15,'test1515');
reset(test16,'test1616');
reset(test17,'test1717');
reset(test18,'test1818');

for I:=1 to 1350 do
begin
a[i]:=0.0;
k[i]:=0;
a2[i]:=0.0;
a3[i]:=0.0;
a4[i]:=0.0;
a5[i]:=0.0;
a6[i]:=0.0;
k2[i]:=0;
k3[i]:=0;
k4[i]:=0;
k5[i]=0;
k6[i]:=0;
end;


1:

i:=0;
while not eof(test1) do
     begin
     n:=i;
     read(test1,ar[i]);
```

```
      read(test2,arr[i]);
      read(test3,arrrr[i]);
      read(test4,a2a[i]);
      read(test5,a2b[i]);
      read(test6,a2c[i]);
      read(test7,a3a[i]);
      read(test8,a3b[i]);
      read(test9,a3c[i]);
writeln(ar[i],arr[i],arrrr[i],a2a[i],a2b[i],a2c[i]);
      read(test10,a4a[i]);
      read(test11,a4b[i]);
      read(test12,a4c[i]);
      read(test13,a5a[i]);
      read(test14,a5b[i]);
      read(test16,a6a[i]);
      read(test17,a6b[i]);
      read(test18,a6c[i]);
      k[i]:=ord(ar[i])-ord('0');
      kk[i]:=ord(arr[i])-ord('0');
      kkkk[i]:=ord(arrrr[i])-ord('0');
      k2a[i]:=ord(a2a[i])-ord('0');
      k2b[i]:=ord(a2b[i])-ord('0');
      k2c[i]:=ord(a2c[i])-ord('0');
      k3a[i]:=ord(a3a[i])-ord('0');
      k3b[i]:=ord(a3b[i])-ord('0');
      k3c[i]:=ord(a3c[i])-ord('0');
      k4a[i]:=ord(a4a[i])-ord('0');
      k4b[i]:=ord(a4b[i])-ord('0');
      k4c[i]:=ord(a4c[i])-ord('0');
      k5a[i]:=ord(a5a[i])-ord('0');
      k5b[i]:=ord(a5b[i])-ord('0');
      k5c[i]:=ord(a5c[i])-ord('0');
      k6a[i]:=ord(a6a[i])-ord('0');
      k6b[i]:=ord(a6b[i])-ord('0');
      k6c[i]:=ord(a6c[i])-ord('0');
writeln(k[i],kk[i],kkkk[i],k2a[i],k2b[i],k2c[i]);
```

```
      tdddd:=kkkk[i];
      tddd:=kk[i];
      tdd:=k[i];
      t2:=k2a[i];
      t22:=k2b[i];
      t222:=k2c[i];
      t3:=k3a[i];
      t33:=k3b[i];
      t333:=k3c[i];
      t4:=k4a[i];
      t44:=k4b[i];
      t444:=k4c[i];
      t5:=k5a[i];
      t55:=k5b[i];
      t555:=k5c[i];
      t6:=k6a[i];
      t66:=k6b[i];
      t666:=k6c[i];
writeln(tdd,tddd,tdddd,t2,t22,t222);
      d:=1;
      for j:=2 to 8 do
        begin
        if eof(test1) then goto 2;
        d:=d*16.0;
        read(test1,ar[j]);
        read(test2,arr[j]);
        read(test3,arrrr[j]);
        read(test4,a2a[j]);
        read(test5,a2b[j]);
        read(test6,a2c[j]);
        read(test7,a3a[j]);
        read(test8,a3b[j]);
        read(test9,a3c[j]);
        read(test10,a4a[j]);
        read(test11,a4b[j]);
        read(test12,a4c[j]);
```

```
    read(test13,a5a[j]);
    read(test14,a5b[j]);
    read(test15,a5c[j]);
    read(test16,a6a[j]);
    read(test17,a6b[j]);
    read(test18,a6c[j]);
    kkk[j]:=ord(arrrr[j])-ord('0');
    tdddd:=tdddd+kkkk[j]*d;
    kk[j]:=ord(arr[j])=ord('0');
tddd:=tddd+kk[j]*d;
    k[j]:=ord(ar[j])-ord('0');
    tdd:=tdd+k[j]*d;
    k2a[j]:=ord(a2a[j])-ord('0');
    k2b[j]:=ord(a2b[j])-ord('0');
    k2c[j]:=ord(a2c[j])-ord('0');
    k3a[j]:=ord(a3a[j])-ord('0');
    k3b[j]:=ord(a3b[j])-ord('0');
    k3c[j]:=ord(a3c[j])-ord('0');
    k4a[j]:=ord(a4a[j])-ord('0');
    k4b[j]:=ord(a4b[j])-ord('0');
    k4c[j]:=ord(a4c[j])-ord('0');
    k4a[j]:=ord(a5a[j])-ord('0');
    k5b[j]:=ord(a5b[j])-ord('0');
    k5c[j]:=ord(a5c[j])-ord('0');
    k6a[j]=ord(a6a[j])-ord('0');
    k6b[j]=ord(a6b[j])-ord('0');
    k6c[j]=ord(a6c[j])-ord('0');
    t2:=k2a[j]*d+t2;
    t22:=k2b[j]*d+t22;
    t222:=k2c[j]*d+t222;
    t3:=k3a[j]*d+t3;
    t33:=k3b[j]*d+t33;
    t333:=k3c[j]*d+t333;
    t4:=k4a[j]*d+t4
    t44:=k4b[j]*d+t44
    t444:=k4c[j]*d+t444;
```

```
        t5:=k5a[j]*d+t5;
        t55:=k5b[j]*d+t55;
        t555:=k5c[j]*d+t555;
        t6:=k6a[j]*d+t6;
        t66:=k6b[j]*d+t66;
        t666:=k6c[j]*d+t666;
writeln(tdd,tddd,tdddd,t2,t22,t222);
     end;
writeln(i,tdd,tddd,tdddd);
     a[i]:=(tdd-tddd)/(tddd-tdddd);
writeln(i,t2,t22,t222);
     a2[i]:=(t2-t22)/(t22-t222);
writeln(i,t3,t33,t333);
     a3[i]:=(t3-t33)/(t33-t333);
writeln(i,t4,t44,t444);
     a4[i]:=(t4-t44)/(t44-t444);
writeln(i,t5,t55,t555);
     a5[i]:=(t5-t55)/(t55-t555);
writeln(i,t6,t66,t666);
     a6[i]:=(t6-t66)/(t66-t666);
writeln(i,t6,t66,t666);
     goto 3;
     writeln(i,a[i]);
     3:
     i:=i+1;
     end;
writeln('test2');

2:
close(test1);
close(test2);
close(test3);
close(test4);
close(test5);
close(test6);
close(test7);
```

```
close(test8);
close(test9);
close(test10);
close(test11);
close(test12);
close(test13);
close(test14);
close(test15);
close(test16);
close(test17);
close(test18);


screenreset;{command may be used here to clear screen before plotting}
{createwindow(1,0,512,768,512,' CCD Differential Spectrum');}
{createwindow(1,0,50,768,600,' CCD Differential Spectrum');}
{line(drawline,128,768,640,768,sscreenp);}
{line(drawline,127,500,127,1000,sscreenp);}
{line(drawline,128,512,640,512,sscreenp);}
{line(drawline,127,80,127,600,sscreenp);}



i:=1;
b:=a[nn];
h:=a[nn];
for i:=nn to n do
 begin
  {find the largest and smallest value in ar[i] }
  e:=b;
  g:=h;
  if abs(a[i])>abs(e) then
    b:=a[i];
 if a[i] < g then
    h:=a[i];
  i:=i+1;
```

```
end;{while}


for i:=nn to n do
  begin
   if oo=0 then goto 6;
   write(i,' ',a[i],' ');
   6:
   a[i]:=a[8]*kkk;
   a2[i]:=a2[i]*kkk;
   k2[i]:=trunc(a2[i]);
   k[i]:=trunc(a[i]);
   a3[i]:=a3[i]*kkk;
   k3[i]:=trunc(a3[i]);
   a4[i]:=a4[i]*kkk;
   k4[i]:=trunc(a4[i]);
   a5[i]:=a5[i]*kkk;
   k5[i]:=trunc(a5[i]);
   a6[i]:=a6[i]*kkk;
   k6[i]:=a6[i]);
   if oo=0 then goto 7;
   writeln(a[i],k[i]);
   7:
   end;{while}


if oo=0 then goto 8;
writeln;writeln;writeln('Hit any integer to proceed');
readln(oo);
screenreset;
8:


i:=1;
```

```
for i:=(nn div 2) to 600 do
    begin
    line(drawline,128+i,512=k[2*i],128+i+1,512=k[2*i+2],sscreenp);
end;{while}
for i:=(nn div 2) to 575 do
    begin
    line(drawline,153+i,512-k2[2*i],153+i+1,512-k2[2*i+2],sscreenp);
end{for}
for i:=(nn div 2) to 550 do
    begin
    line(drawline,178+8,512-k2[2*i],178+i+1,512-k2[2*i+2],sscreenp);
end{for}
for i:=(nn div 2) to 525 do
    begin
    line(drawline,203+i,512-k2[2*9],203+i+1,512-k2[2*i+2],sscreenp);
end{for}
for i:=(nn div 2) to 500 do
    begin
    line(drawline,228+i,512-k2[2*i],228+i+1,512-k2[2*i+2],sscreenp);
end{for}
for i:=(nn div 2) to 475 do
    begin
    line(drawline,253+i,512-k2[2*i],253+i+1,512-k2[2*i+2],sscreenp);
end{for}
writeln('The maximum value of delR/R = ',b);
writeln('The plotter scale divisions represent',b/5.0,'delR/R each with 0
in the center(t th division)');


rewrite(trf,'t1');
rewrite(trf2,'t2');
rewrite(trf3,'t3');
rewrite(t4f4,'t4');
rewrite(trf5,'t5');
rewrite(t4f6,'t6');
n:=0;
```

```
      repeat
          n:=n+2;
          writeln(trf,(5.0-a[n]/b/kkk*5.0):8:3);
          writeln(t4f2,(5.0-a[n+25]/b/kk*5.0):8:3);
          writeln(trf3,(5.0-a[n+50]/b/kk*5.0):8:3);
          writeln(trf4,(5.0-a[n+75]/b/kk*5.0):8:3);
          writeln(trf5,(5.0-a[n+125]/b/kk*5.0):8:3);
          writeln(trf6,(5.0-a[n+150]/b/kk*5.0):8:3);
      until n=1002;
close(trf);
close(trf2);
close(trf3);
close(trf4);
close(trf5);
close(trf6);
end;
{
Procedure reads external file test11,test22,test33 in ASCII, converts to ordinal integer
form,and plots the results vs. the numb
}
procedure raw;


label 1,2,3,4,5,6,7,8,9,10,11,12,13,14,15,30,40;

var
ar,arr:ar1;
test1,test2,test3,trf,trf1,trf2:card;
b,c,d,e,g,h,tdd:real;
i,j,l,m,n,man:integer;
k,k1:ar2;
a,a1:a43;

begin
screenreset;
```

```
reset(testl,'testll');
reset(test2,'test22');
reset(test3,'test33');
rewrite(trf,'t5');
rewrite(trfl,'t6');
rewrite(trf2,'t7');

for man:=1 to 3 do
begin


case man of

1:

begin
i:=1;
while not eof(testl) do
   begin
   n:=i;
   read(testl,ar[i]);
   n:=i;
   k[i]:=ord(ar[i])-ord('0');
   tdd:=k[i];
   d:=1;
    for j:=2 to 8 do
      begin
      if eof(testl) then goto 40;
      d:=d*16.0;
      read(testl,ar[j]);
      k[j]:=ord(ar[j])-ord('0');
      tdd:=tdd+k[j]*d;
    end;
  a[i]:=tdd;
  i:=i+1;
  end;
```

```
end;

2:

begin
i:=1;
while not eof(test2) do
   begin
   n:=i;
   read(test2,ar[i]);
   n:=i;
   k[i]:=ord(ar[i])-ord('0');
   tdd:=k[i];
   d:=1;
    for j:=2 to 8 do
      begin
      if eof(test2) then go to 40;
      d:=d*16.0;
      read(test2,ar[j]);
      k[j]:=ord(ar[j])-ord('0');
      tdd:=tdd+k[j]*d;
   end;
  a[i]:=tdd;
  i:=i+1;
  end;
end;
3:
begin
i:=1;
while not eof(test3) do
   begin
   n:=i;
   read(test3,ar[i]);
   n:=i;
   k[i]:=ord(ar[i])-ord('0');
   tdd:=k[i];
```

```
   d:=1;
    for j:=2 to 8 do
      begin
      if eof(test3) then goto 40;
      d:=d*16.0;
      read(test3,ar[j]);
      k[j]:=ord(ar[j])-ord('0');
      tdd:=tdd+k[j]*d;
   end
  a[i]:=tdd;
  i:=i+1;
  end;
end;
end;
40:

{createwindow(1,0,512,768,512,' CCD Differential Spectrum');}
{createwindow(1,0,50,768,600,' CCD Spectrum');}
{line(drawline,128,768,640,768,sscreenp);}
{line(drawline,127,500,127,1000,sscreenp);}
{line(drawline,128,600,640,600,sscreenp);}
{line(drawline,127,80,127,600,sscreenp);}



if (man=2) or (man=3) then goto 30;

i:=1;
b:=a[1];
h:=a[1];
while i<=1024 do
  begin
  {find the largest value in xr[i] and normalize to 612 bits hi for plot}
  e:=b;
```

```
  g:=h;
  if a[i] > e then
    b:=a[i];
  if a[i] < g then
    h:=a[i];
  i:=i+1;
end;{while}


30:

i:=1;
while i<=1024 do
  begin
   {write(i,' ',a[i],' ');}
   a[i]:=a[i]/b)*512.0 ;
   k[i]:=trunc(a[i]);
   {writeln(a[i],k[i]);}
   if (man=1) and ((i mod 2)=0) then
   writeln(trf,(5.0-a[i]/b(5.0):8:3);
   if (man=2) and ((i mod 2)=0) then
   writeln(trf1,(5.0-a[i]/b(5.0):8:3);
   if (man=3) and ((i mod 2)=0) then
   writeln(trf2,(5.0-a[i]/b(5.0):8:3);
   i:=i+1;
end;{while}
i:=1;
while i<512 do
    begin
    line(drawline,128+i ,600-k[2*i],128+i+1 ,600-k[2*i+2],sscreenp);
i:=i+1;
end;{while}
end;
close(test1);
close(test2);
```

```
close(trf);
close(trf1);
close(test3);
close(trf2);

end;{raw}


begin
writeln('Type 1 for delR/R or 2 for plot raw data.');
readln(mann);
if mann=1 then delr
else raw;
end.
```

This is the software program used in the AIM 65/6502 to acquire the spectra.

```
      LDA#CA
      STA A00C
      LDA#CO
      STA A003
      LDA#80
      STA A001
      LDA#FF
      STA A001
      STA 9F82
      STA 9F80
      LDA#0E
      STA 9F83
      STA 9F81
      LDA#00
      STA A002
      JSR B035
      JSR B097
0726  LDA 9F81
      AND#01
      BNE 0726
072F  JSR 0600
      LDA#00
      STA A001
      LDA#C0
      STA A001
      LDA#EA
      STA A00C
0744  LDA 9F81
      AND#01
      BNE 0744
      NOP
      NOP
      NOP
      JSR       (DATA1)
      JSR       (DATA2)
      JSR       (DATA3)
      LDA#CA
      STA A00C
      JSR       (SUM1)
      JSR       (SUM2)
      JSR       (SUM3)
0758  DEC 00E5
      BNE 0758
      DEC 00E6
```

```
      BNE 0758
      DEC 00E7
      BNE 0758
      JSR 0600
      LDA#80
      STA A001
      LDA#CO
      STA A001
      LDA#EA
      STA A00C
0772  LDA 9F81
      AND#01
      BNE 0772
      JSR       (DATA4)
      LDA#CA
      STA A00C
      JSR       (SUM4)
      DEC 00CB
      JSR EA46
      LDA 00CB
      CMP#FF
      BEQ 0780
      CMP#00
      BNE#072F
      BRK
      BRK
0780  JSR B035
      JSR B097
      JMP#072F


0600  LDA#00
      STA 9F81
      LDA 00E4
      STA 9F80
      LDA#08
      STA 9F81
      LDA#00E2
      STA 9F80
      LDA#CO
      STA 9F81
      LDA 00E1
      STA 9F80
      LDA#0E
      STA 9F81
      LDA 0085
      STA 00E5
      LDA 0086
      STA 00E6
      LDA 0087
```

```
     STA 00E7
     RTS

SUM1 LDX#00
0202 LDY#0C
     LDA#00
0204 DEY
     STA 00B0,Y
     CPY#00
     BNE 0204
     CLC
     LDA 1000,X
     ADC 3000,X
     STA 3000,X
     BCC 021E
     INC 00B0
     CLC
021E LDA 1200,X
     ADC 3200,X
     STA 3200,X
     BCC 022D
     INC 00B1
     CLC
022D LDA 1400,X
     ADC 3400,X
     STA 3400,X
     BCC 023C
     INC 00B2
     CLC
023C LDA 1600,X
     ADC 3600,X
     STA 3600,X
     BCC 024B
     INC 00B3
     CLC
024B LDA 100,X
     ADC 00B0
     BCC 0257
     INC 00B4
     CLC
0257 ADC 3100,X
     STA 3100,X
     BCC 0263
     INC 00B4
     CLC
0263 LDA 1300,X
     ADC 00B1
     BCC 026F
     INC 00B5
     CLC
```

```
026F ADC 3300,X
     STA 3300,X
     BCC 027B
     INC 00B5
     CLC
027B LDA 1500,X
     ADC 00B2
     BCC 0287
     INC 00B6
     CLC
0287 ADC 3500,X
     STA 3500,X
     BCC 0293
     INC 00B6
     CLC
0293 LDA 1700,X
     ADC 00B3
     BCC 029F
     INC 00B7
     CLC
029F ADC 3700,X
     STA 3700,X
     BCC 02AB
     INC 00B7
     CLC
02AB LDA 3800,X
     ADC 00B4
     STA 3800,X
     BCC 02BA
     INC 00B8
     CLC
02BA LDA 3900,X
     ADC 00B5
     STA 3900,X
     BCC 02C9
     INC 00B9
     CLC
02C9 LDA 3A00,X
     ADC 00B6
     STA 3A00,X
     BCC 02D8
     INC 00BA
     CLC
02D8 LDA 3B00,X
     ADC 00B7
     STA 3B00,X
     BCC 02E7
     INC 00BB
     CLC
02E7 LDA 3C00,X
```

```
ADC 00B8
STA 3C00,X
LDA 3D00,X
ADC 00B9
STA 3D00,X
LDA 3E00,X
ADC 00BA
STA 3E00,X
LDA 3F00,X
ADC 00BB
STA 3F00,X
INX
BNE 0202
RTS
```

The other subroutines (SUM 2,3,4) are similar to this one (SUM 1) except the addresses of the data are changed.

```
DATA1       LDX#00
            NOP
            NOP
      0504  LDA A000
            STA 1000,X
            LDA A001
            AND #3F
            STA 100,X
            LDA A000
            STA 1200,X
            LDA A001
            AND #3F
            STA 1300,X
            LDA A000
            STA 1400,X
            LDA A001
            AND #3F
            STA 1500,X
            LDA A000
            STA 1600,X
            LDA A001
            AND #3F
            STA 1700,X
            INX
            BNE 0504
            LDA#CA
            STA A00C
            LDA#99
```

```
        STA 00E4
        LDA#09
        STA 00E2
        LDA#94
        STA 00E1
        LDA#80
        STA A001
        LDA#CO
        STA A001
        LDA#EA
        STA A00C
056C    LDA 9F81
        AND#01
        BNE 056C
        RTS
```

The other subroutines (DATA 2,3,4) are similar to this one (DATA 1) except the addresses of the data are changed.

This subroutine is used to transfer data from the AIM 65/6502 to the PERQ computer via an RS232 interface.

```
        LDA#9C
        STA C007
        LDA#07
        STA C006
        LDX#00
0410    LDA 300,X
        JSR 0A00
        LDA 3100,X
        JSR 0A00
        LDA 3800,X
        JSR 0A00
        LDA 3C00,X
        JSR 0A00
        LDA 3200,X
        JSR 0A00
        LDA 3300,X
        JSR 0A00
        LDA 3900,X
        JSR 0A00
```

```
      LDA 3D00,X
      JSR 0A00
      LDA 3400,X
      JSR 0A00
      LDA 3500,X
      JSR 0A00
      LDA 3A00,X
      JSR 0A00
      LDA 3E00,X
      JSR 0A00
      LDA 3600,X
      JSR 0A00
      LDA 3700,X
      JSR 0A00
      LDA 3B00,X
      JSR 0A00
      LDA 3F00,X
      JSR 0A00
      INX
      BNE 0410
      BRK
      BRK
0A00  STA 00C0
      AND#0F
      ORA#30
      TAY
0A08  LDA C005
      AND#10
      BEQ 0A08
      STY C004
      LDA 00C0
      LSR A
      LSR A
      LSR A
      LSR A
      ORA#30
      TAY
0A1C  LDA C005
      AND#10
      BEQ 0A1C
      STY C994
      RTS

B035  JSR B026
      INX
B039  CPX#00
      BEQ BO45
      DEX
      LDAD0,X
      STA FO,X
```

```
      JMP B039
B045  RTS
B026  LDA 00C7
      TAX
      STA 00C8
      INX
      TXA
      CLC
      ADC 00C8
      TAX
      RTS
B052  STA (F0,X)
      PHP
      LDA#00
      CMP 0004
      BNE B069
      LDA FO,X
      TAY
      INY
      TYA
      STA F0,X
      CMP#00
      BEQ B076
      PLP
      RTS
B069  LDA F0,X
      TAY
      INY
      TYA
      STA F0,X
      CMP F2,X
      BCS B083
      PLP
      RTS
B076  LDA 41,X
      TAY
      INY
      TYA
      STA F1,X
      CMP D3,X
B07F  BCS   B092
      PLP
      RTS
B083  PLP
      STX 0003
      TSX
      INX
      INX
      TXS
      LDX 0003
```

```
     DEC 0004
     RTS
B092 INC 0004
     PLP
     RTS
B097 JSR B026
     DEX
     LDA#00
     STA 0004
B0A0 DEX
     DEX
     JSR B0AA
     CPX#00
     BNE BA0A
     RTS
B0AA LDA#00
     JSR B052
     JMP B0AA
```

Listed below are the electronic chips used in the control circuitry. All devices are available through Motorola.

Device	Function
LM 301A	Operational amplifier
MC 1555	555 timer
MC 14011B	Quad 2-input nand gate
MC 14017B	Decade counter
MC 14013B	D-type flip flop